# On the timing and nature of magmatism in the North Atlantic Igneous Province: New implications from basaltic rocks of the Faroe Islands

**Jógvan Hansen[a]*, Morgan Ganerød[b]**

[a]Independent researcher. Rygsgøta 8, FO 370 Midvag, Faroe Islands
[b]Norges Geologiske Undersøkelse, Leiv Eirikssons vei 39, 7040 Trondheim, Norway
*Corresponding author: jogvan.hansen@dunelm.org.uk; jogvanha@olivant.fo

## Abstract

New $^{40}Ar/^{39}Ar$ ages representing a number of basaltic sills and a key lava flow from the Faroe Islands are presented in this contribution and utilised in order to assess the igneous history of parts of this region. In turn, the acquired ages are contrasted against other Faroese rocks of known ages as well as against other comparable igneous regions in the North Atlantic area. Altogether, the novel ages obtained in this work enable us to put new constraints on the timing of late stage magmatic activity and hence lithospheric extension within this part of the North Atlantic Igneous Province, which the Faroe Islands form part of. Even though the main stages of igneous activity within the North Atlantic Igneous Province generally took place within a time span of ~61 Ma to ~55 Ma, examples of more recent magmatism have been documented for W Greenland, E Greenland, the Norwegian – Greenland Sea, igneous centres at the eastern fringes of the Rockall Plateau and in the Rockall trough, thus testifying that lithospheric extension off rift axes continued for some noticeable time following onset of regional seafloor spreading. In this research we present new ages as young as ~50.5 Ma for some of the smallest Faroese sills and demonstrate that the larger and oldest sills of the Faroe Islands, grouped into the Streymoy/Kvívík sills and the Eysturoy/Sundini sills respectively (~55.5 Ma), likely formed just subsequent to the formation of the uppermost parts of the Enni Formation, which represent the latest stages of local surface magmatism at ~55.8 Ma. Gradually decreasing volumes of Faroese sills coupled with sequentially younger ages point to systematic decrease of local igneous activity with increasing distances to active regional rifting zones in the Early Paleogene Period, as the young Faroese lava plateau gradually drifted away from the then active regional rift axis. Similar scenarios in other parts of the North Atlantic Igneous Province support our inferences that it was commonplace within this large igneous province to experience relatively small-scale lithospheric extension and magmatism at some distances from zones/axes of active seafloor-spreading. Age variations between igneous products of the Faroe Islands versus those of the central E Greenland point to a somewhat diacronous evolution pattern within this part of the North Atlantic Igneous Province subsequent to ~57.5 Ma. Accordingly, our study does not preclude the existence of a contemporaneous Icelandic microcontinent between Faroe Islands and central E Greenland.

Keywords: Faroe Islands; $^{40}Ar/^{39}Ar$ geochronology; Geochemistry; Low-$TiO_2$ and high-$TiO_2$ basalts; Basaltic rocks; North Atlantic Igneous Province; Large Igneous Province

## 1. Introduction

The basaltic rocks building up the archipelago of the Faroe Islands Basalt Group (FIBG) form part of the North Atlantic Igneous Province (NAIP), which itself is one of the Large Igneous Provinces (LIPs) on Planet Earth (Saunders et al., 1997; Saunders, 2016). Combined, the igneous regions of the NAIP encompass a vast area in the North Atlantic with igneous products to be found in the eastern parts of the Baffin Island, in West Greenland, in East

Greenland, offshore West Norway (Vøring and Møre basins), in the Faroe Islands, on the Rockall Plateau and in the NW British Isles (Wilkinson et al., 2016) (Fig. 1). More recent additions of igneous products to the NAIP occurred in Iceland and the adjacent submerged Greenland-Iceland and Iceland-Faroes ridges, on smaller scales in Jan Mayen, in West and East Greenland, in submerged igneous complexes/seamounts in the Norwegian-Greenland Sea, on either side of the Reykjanes ridge, on top of and on the eastern fringes of the Rockall Plateau and in the Rockall Trough (Hansen et al., 2009; Hansen, 2011; Wilkinson et al., 2016; Á Horni et al., 2017).

Magmatic events within the various igneous regions of the NAIP have traditionally been associated with incipient lithospheric extension in the Early Paleogene Period along axes in the Labrador Sea, offshore East Greenland and in the Rockall Trough through the Shetland Basin respectively, followed by active extension-related seafloor-spreading in the NE Atlantic and in the Labrador Sea (Saunders et al., 1997; Meyer et al., 2007; Hansen et al., 2009; Millet et al., 2020). Hence, reliable radiometric age determinations of representative igneous products within the various parts of the NAIP are of utmost importance in order to determine the magmatic development along the various extension/rift axes within this LIP in order to evaluate the timing of lithospheric stretching in the various igneous regions prior to, contemporaneous to and subsequent to initiation of active seafloor spreading.

In this contribution we present novel $^{40}Ar/^{39}Ar$ ages for a number of basaltic sills intruded into the lava succession of the Faroe Islands and for a key local lava flow. The obtained new radiometric ages are in turn utilised in order to assess the igneous evolution locally within the actual region in addition to being briefly contrasted against some radiometric ages of other parts of the NAIP, so as to evaluate their proper place within the broader context of the entire igneous province.

## 2. Regional Geology

Being situated between East Greenland and the NW European continental margin, the Faroe Island Basalt Group (FIBG) makes up a relatively central part of the NAIP (Fig. 1). The exposed onshore parts of the Faroese basaltic lava pile cover around 1400 km$^2$ with a total stratigraphic extent (exposed and drilled) of around 6,6 km (Hansen et al., 2019 and refs. therein). The Faroese lava pile is grouped into seven formations being from bottom and up: the ~1075 m thick Lopra Formation; the ~3250 m thick Beinisvørð Formation; the ~9 m thick Prestfjall Formation; the 40-50 m thick Hvannhagi Formation; the 1250-1350 m thick Malinstindur Formation; the ~30 m thick Sneis Formation and finally the ~900 m thick Enni

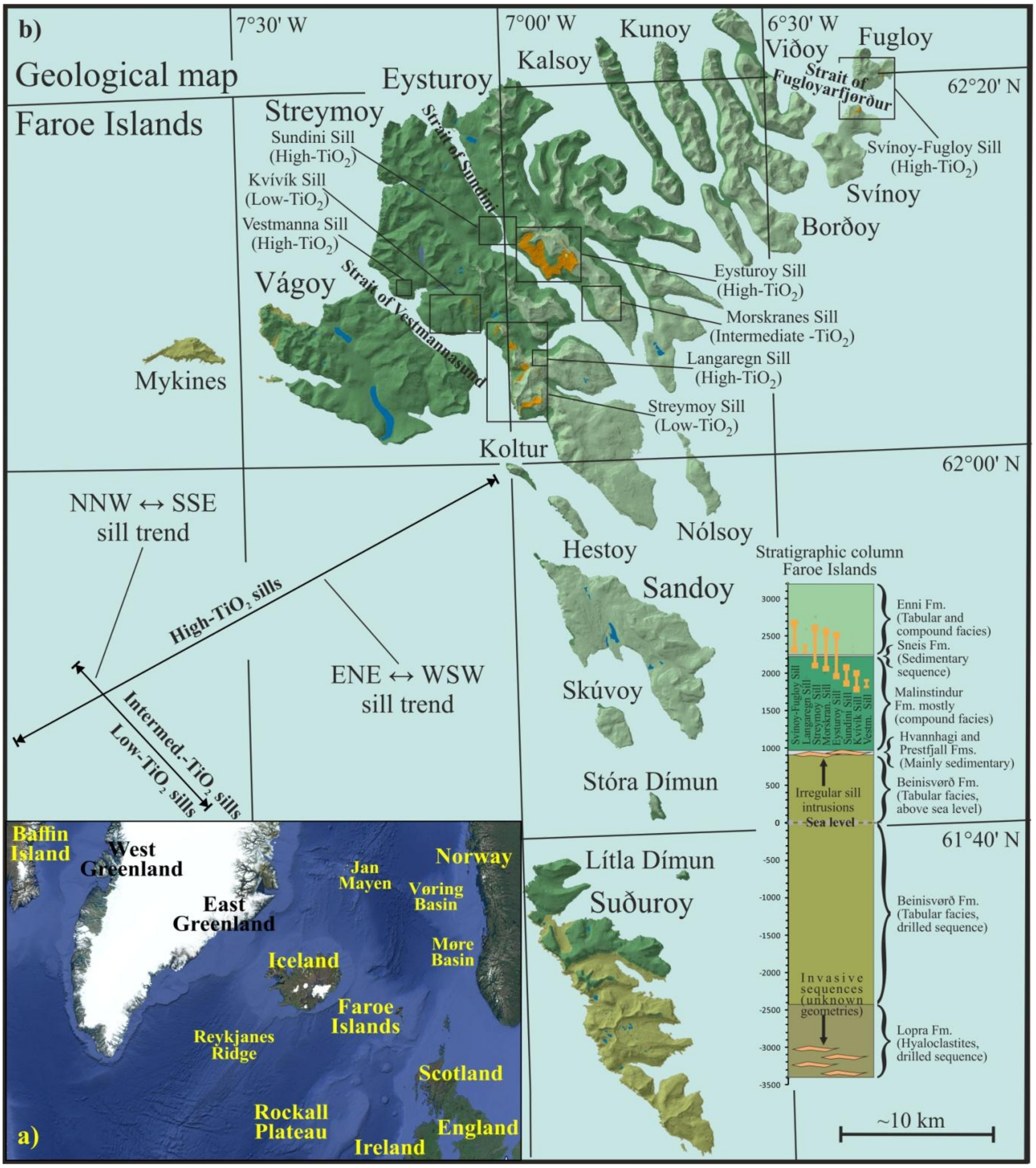


**Figure 1.** Maps showing the area relevant for this study. a) The "Google Earth" based map illustrates locations of the main parts of the NAIP, including the focus of this study the Faroe Islands. b) The map, based on topographic data from Munin Fo, shows the main basaltic formations building up the Faroe Islands (Modified from Hansen, 2011; Hansen et al., 2011; Hansen et al., 2019; Hansen, 2020). The stratigraphic column illustrates the thicknesses of the various geological formations according to nomenclature of Passey and Jolley (2009). Orange bars indicate total vertical (stratigraphic) extent of the actual sills. Simplistic explanation on general sill trends and extents are shown on central left of b).

Formation (Passey and Jolley, 2009) (Fig. 1). In addition to the entire Faroese lava pile being intruded by numerous large sub-vertical dykes of various thicknesses, the Malinstindur, Sneis

and Enni formations are intruded by a few basaltic transgressive (saucer-shaped) sills of various extent and thicknesses, which probably represent the latest manifestations of igneous activity within the actual region (Hansen et al., 2011; Hansen, 2015; Hansen et al., 2019).
A number of attempts to estimate/measure the age(s) of lavas of the Faroe Islands have been undertaken previously, including paleomagnetic dating (Tarling and Gale, 1968; Waagstein, 1988; Abrahamsen, 2006 and refs. therein), palynologic age estimates (Jolley and Bell, 2002) and radiometric $^{40}Ar/^{39}Ar$ dating (Waagstein et al., 2002; Storey et al. 2007). Out of these, the most recent age determinations by Storey et al. (2007) appear to be most reliable and are to a large extent consistent with ages of comparable basaltic lavas from other regions of the NAIP. The age determinations by Storey et al. (2007) prior to any update/corrections indicate ages of ~60 Ma for the bottom of the Beinisvørð Formation and ~57 Ma for its top sections, while they measured an age of ~55.2 Ma for the upper parts of the preserved lava successions of the Enni Formation (corrected/adjusted ages are shown in Fig. 4).

## 3. Results

### *3.1. Sampling and petrography*

Initially, samples were collected from 7 Faroese sills (the Streymoy, Kvívík, Eysturoy, Morskranes, Svínoy-Fugloy, Langaregn and Vestmanna sills) and a key Faroese lava flow (bottom of the Malinstindur Formation). Noticeable proportions of the exposed parts of the Faroese sills are intensely jointed and/or have been exposed to chemical weathering. As the main bodies of individual Faroese sills display quite homogeneous petrography and geochemistry (Hansen, 2011; Hansen et al., 2019), the foremost criterion involved in the actual sampling was the choosing of absolutely fresh specimen. Hence, great care has been taken in this research project to collect representative sill samples without joints or visible signs of weathering at the whole-rock scale. Similar precautions were taken during collection of the local lava sample. General petrography and geochemistry for the bulk of Faroese sills and lavas have been detailed in previous studies (Holm et al., 2001, Hansen, 2011, Hansen et al., 2019).
The actual $^{40}Ar/^{39}Ar$ analyses are mostly based upon groundmass material, whilst plagioclase was used for a couple of samples. Sample qualities at the whole-rock scale were assessed on thin-sections (microscopy) and on major elements determined by means of X-ray fluorescence (XRF) analyses.

### *3.2. Analytical techniques*

All samples were crushed and sieved to obtain 180 – 250 μm fractions. The finer particles were decanted in tap water and the coarser residue further ultrasonically washed in acetone and de-ionized water several times. The grains deemed by optical investigations to be best suited, being void of any coatings, were handpicked under a stereomicroscope. The samples were packed in aluminium capsules together with the Taylor Creek Rhyolite (TCR) flux monitor standard along with zero age reagent grade $K_2SO_4$ and optical grade $CaF_2$ salts for interference corrections. The samples were irradiated at the MTA reactor (Hungary) for c. 2 hours, with a nominal fast neutron flux density of c. $5.5\times10^{13}$ n*(cm$^{-2}$ *s$^{-1}$). The interference correction factors for the production of isotopes from Ca and K are shown in Table 1. Groundmass and plagioclase materials were placed in a 3.5mm pit size aluminium sample disk and step heated using a defocused 3.5 mm $CO_2$ laser beam from Photon Machine Fusions 10.6 with a flat energy spectrum. The extracted gases from the sample cell were expanded into a Piston Free Stirling Cryocooler for trapping potential water vapour and further into a two-stage low volume extraction line (c. 300 cm$^3$), both stages equipped with SAES GP-50 (st101 alloy) getters, the first running hot (c. 350 °C) and the second running at room temperature. The samples were analyzed with a MAP 215–50 mass spectrometer in static mode, installed at the Geological Survey of Norway. The peaks and baseline (AMU = 36.2) were determined during peak hopping for 15 cycles (15 integrations per cycle, 30 integrations on mass $^{36}$Ar) on the different masses ($^{40–36}$Ar) on a MasCom electron multiplier (MC217) in analogue mode and linearly regressed back to zero inlet time. Blanks were analyzed every third measurement. After blank correction, a correction for mass fractionation, $^{37}$Ar and $^{39}$Ar decay and neutron-induced interference reactions produced in the reactor was undertaken using in-house software AgeMonster, written by M. Ganerød. It implements the equations of McDougall and Harrison (1999) and the recently proposed decay constant for $^{40}$K after Renne et al. (2010). A $^{40}$Ar/$^{36}$Ar ratio of 298.56 ± 0.31 from Lee et al. (2006), was used for the atmospheric argon correction and mass discrimination calculation using a power law distribution of the masses. We calculated J-values (irradiation flux parameter) relative to an age of 28.619 ± 0.036 Ma for the TCR fluence monitor (Renne et al., 2010). We used the following criteria to determine the sample ages: at least 3 overlapping consecutive steps (95% confidence), accounting of more than 50% cumulative $^{39}$Ar released from the spectra analyses.

**Table 1.** Early Cenozoic $^{40}Ar/^{39}Ar$ ages representing sills and lavas of the Faroe Islands.

| | | | | Spectra | | | | Inverse isocron | | |
|---|---|---|---|---|---|---|---|---|---|---|
| Lavas and sills | Sample | Material | Steps (n) | %$^{39}Ar$ | Age ± 1.96s Ma | MSWD (P) | K/Ca ± 1.96s | Age ± 1.96s | MSWD (P) | Trapped $^{40}Ar/^{36}Ar$ |
| Streymoy Sill | SS1 | Groundmass | 7-18(12) | 57.09 | 55.31 ± 4.53 | 0.15(1.00) | 0.06426 ± 0.00179 | 54.00 ± 8.18 | 0.15(1.00) | 304.75 ± 33.30 |
| Kvívík Sill | 17-JKS-01 | Groundmass | 2-11(10) | 84.22 | 55.45 ± 2.83 | 0.73(0.68) | 0.04452 ± 0.00170 | 56.27 ± 6.29 | 0.82(0.59) | 297.47 ± 7.92 |
| Eysturoy Sill | ES-1 | Plagioclase | 5-11(7) | 36.89 | 55.20 ± 1.37 | 1.11(0.35) | 0.07 ± 0.00 | 54.36 ± 3.91 | 1.29(0.27) | 309.89 ± 48.72 |
| Eysturoy Sill | ES-2 | Groundmass | 14-20(7) | 64.52 | 55.52 ± 1.25 | 0.88(0.50) | 0.05970 ± 0.00241 | 55.31 ± 11.77 | 1.06(0.38) | 299.62 ± 59.73 |
| Svínoy-Fugloy Sill | FS-1 | Groundmass | 2-9(8) | 74.54 | 54.06 ± 1.89 | 1.25(0.27) | 0.08418 ± 0.00271 | 59.40 ± 6.33 | 1.06(0.39) | 275.21 ± 28.32 |
| Svínoy-Fugloy Sill | FS-2 | Groundmass | 4-13(10) | 48.63 | 54.76 ± 3.56 | 0.27(0.98) | 0.03 ± 0.00 | 52.75 ± 14.93 | 0.29(0.97) | 306.51 ± 62.50 |
| Morskranes Sill | 17-JMS-01 | Groundmass | 4-13(10) | 70.34 | 53.16 ± 3.90 | 0.35(0.96) | 0.02 ± 0.00 | 56.77 ± 11.48 | 0.35(0.95) | 291.14 ± 23.60 |
| Langaregn Sill | 18-JLRS-01 | Groundmass | 9-20(12) | 63.18 | 50.72 ± 1.25 | 0.91(0.53) | 0.02909 ± 0.00096 | 39.79 ± 9.13 | 0.39(0.95) | 342.72 ± 39.38 |
| Vestmanna Sill | 16-JVEST-02 | Plagioclase | 2-9(8) | 56.79 | 50.31 ± 1.59 | 0.94(0.47) | 0.00372 ± 0.00003 | 58.69 ± 8.02 | 0.49(0.82) | 286.12 ± 12.12 |
| Malinstindur FM | 16-JHVAL-02 | Groundmass | 6-18(13) | 81.51 | 56.34 ± 1.87 | 1.40(0.16) | 0.07827 ± 0.00349 | 50.95 ± 3.72 | 0.57(0.85) | 318.20 ± 12.47 |

Ages are reported relative to Sanidine standard TRC (28.619 ± 0.036 Ma, Renne et al., 2010). n = number of heating steps used/total. Age, weighted by the inverse of variance. MSWD, mean square of weighted deviations.

### *3.3. Results*

The range of $^{40}Ar/^{39}Ar$ ages determined for the sills of this study span from ~50.3 Ma to ~55.5 Ma, i.e. a total time interval of ~5 million years, while the age of the single local lava flow is ~56.34 Ma (Table 1; Figure 2). Combined, the Faroese sills formed at relatively irregular intervals (Figure 2). The Streymoy, Kvívík and Eysturoy sills, which amongst themselves belong to two distinct geochemical groups (the low-$TiO_2$ Streymoy/Kvívík sills and the high-$TiO_2$ Eysturoy/Sundini sills respectively), formed at 55.2 to 55.5 Ma; the High-$TiO_2$ Svínoy-Fugloy Sill was emplaced at 54.1 to 54.8 Ma; the intermediate-$TiO_2$ Morkranes sill came into being at ~53.2 Ma while the high-$TiO_2$ Langaregn and Vestmanna sills formed at 50.3 to 50.7 Ma. There are clear and systematic changes in sill sizes/volumes in accordance with their measured ages. The oldest local sills (at ~55.35 Ma on average) display the largest volumes whereas the slightly younger Svínoy-Fugloy Sill (at ~54.45 Ma on average) is noticeably less bulky; the Morskranes Sill (at ~53.2 Ma) in turn is smaller than the Svínoy-Fugloy Sill, while the Langaregn and Vestmanna sills (at ~50.5 Ma on average) are considerably less voluminous than all other local sills (Hansen, 2011; Hansen et al., 2011). Apart from the two local sill groups consisting of the low-$TiO_2$ Streymoy and Kvívík sills and the high-$TiO_2$ Eysturoy and Sundini sills respectively, which display identical geochemical compositions within each group, the Faroese sills in general originate from somewhat heterogeneous mantle sources (Hansen, 2011; Hansen et al., 2019). Hence, supposed extension within the mantle (sub-continental lithospheric mantle [SCLM]?), which presumably triggered sporadic igneous activity within the actual area at ~55.5 to ~50.5 Ma, affected several geochemically different mantle reservoirs during this period of time.

**Figure 2** (next page)**.** Age spectra for seven basaltic sills and one selected local lava flow of the Faroe Islands from Table 1. Individual plateau ages (± 1.96σ), presented according to interpretations of individual steps versus cumulative % $^{39}Ar$ release, are indicated on individual part figures. Individual incremental-heating steps (boxes), used for age determinations are indicated in grey colour. Associated K/Ca and % radiogenic $^{40}Ar$ versus cumulative % $^{39}Ar$ release diagrams are presented in electronic Supplement A (Hansen and Ganerød, 2021). a) and b) represent two samples of the High-$TiO_2$ Eysturoy Sill; c) and d) represent two samples of the low-$TiO_2$ Streymoy and Kvívík sills respectively; e) and f) represent two samples from the high-$TiO_2$ Svínoy-Fugloy Sill; g) represents the intermediate-$TiO_2$ Morskranes Sill while h) and i) represent the high-$TiO_2$ Langaregn and Vestmanna sills respectively. j) represents lava flows of the bottom of the local Malinstindur Formation.

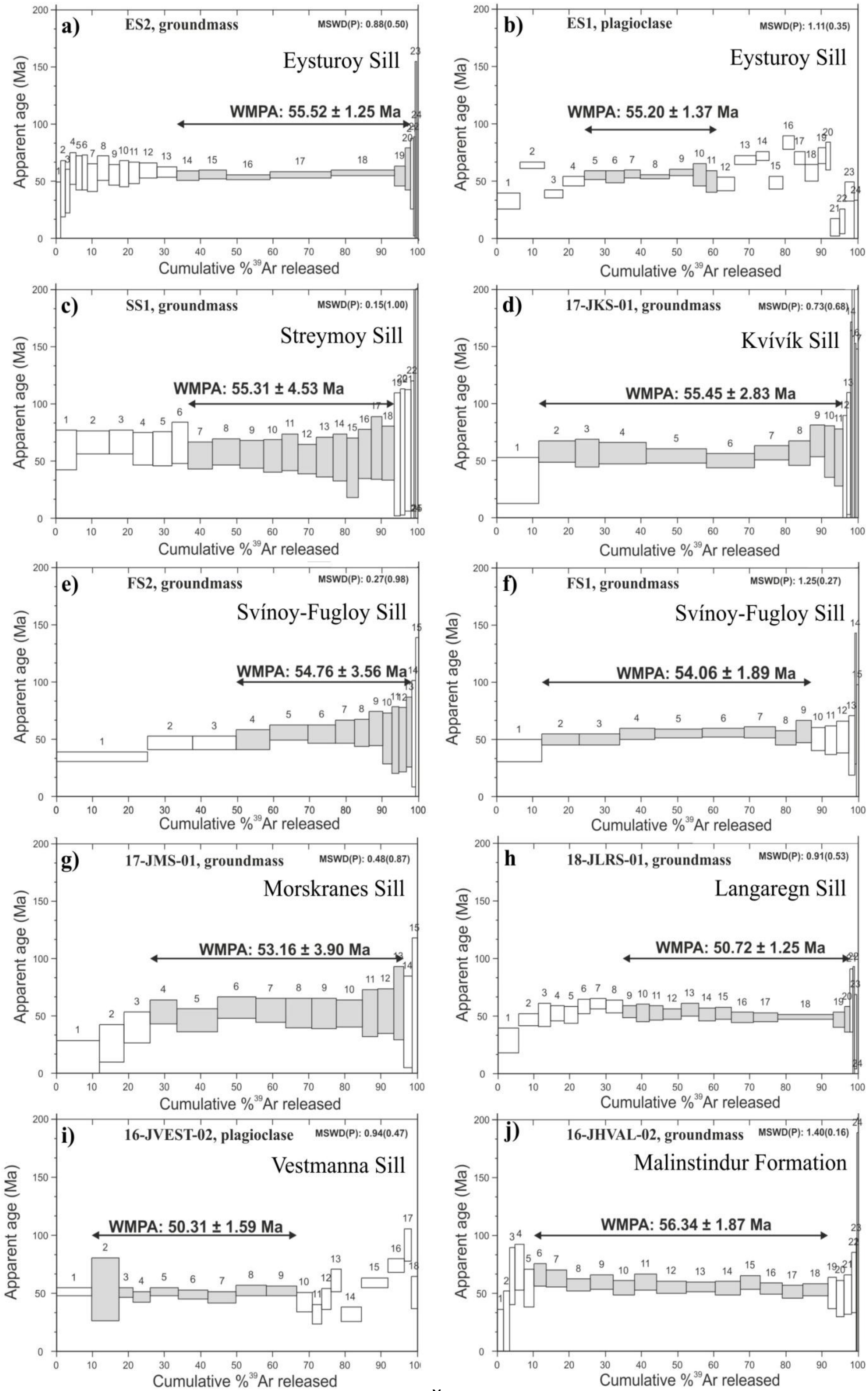
a)
ES2, groundmass
MSWD(P): 0.88(0.50)
Eysturoy Sill
WMPA: 55.52 ± 1.25 Ma
b)
ES1, plagioclase
MSWD(P): 1.11(0.35)
Eysturoy Sill
WMPA: 55.20 ± 1.37 Ma
c)
SS1, groundmass
MSWD(P): 0.15(1.00)
Streymoy Sill
WMPA: 55.31 ± 4.53 Ma
d)
17-JKS-01, groundmass
MSWD(P): 0.73(0.68)
Kvívík Sill
WMPA: 55.45 ± 2.83 Ma
e)
FS2, groundmass
MSWD(P): 0.27(0.98)
Svínoy-Fugloy Sill
WMPA: 54.76 ± 3.56 Ma
f)
FS1, groundmass
MSWD(P): 1.25(0.27)
Svínoy-Fugloy Sill
WMPA: 54.06 ± 1.89 Ma
g)
17-JMS-01, groundmass
MSWD(P): 0.48(0.87)
Morskranes Sill
WMPA: 53.16 ± 3.90 Ma
h
18-JLRS-01, groundmass
MSWD(P): 0.91(0.53)
Langaregn Sill
WMPA: 50.72 ± 1.25 Ma
i)
16-JVEST-02, plagioclase
MSWD(P): 0.94(0.47)
Vestmanna Sill
WMPA: 50.31 ± 1.59 Ma
j)
16-JHVAL-02, groundmass
MSWD(P): 1.40(0.16)
Malinstindur Formation
WMPA: 56.34 ± 1.87 Ma
Apparent age (Ma)
Cumulative %39Ar released

## 4. Discussion

### *4.1. Basic remarks*

Measured and recalculated ages representing Faroese lava formations fall well within age ranges measured for similar lava successions of other igneous regions of the NAIP such as W Greenland, E Greenland NW British Isles and sills of the Vøring Basin, offshore Norway (Hansen et al., 2009 and refs. therein; Tegner et al., 2008; Ganerød et al., 2010; Svensen et al., 2010; Brooks, 2011 and refs. therein; Larsen et al., 2016; Wilkinson et al., 2016 and refs. therein; Franke et al., 2019). Ages recorded for the Faroese Malinstindur and Enni formations (Fig. 4) in this contribution straddle the proposed/estimated timeline of incipient 'main' opening phase of the North Atlantic at ~56 Ma to 55.6 Ma (e.g. Wilkinson et al., 2016) and likely formed in association to this momentous event. Interestingly, a number of relatively recent research and reviews on evolutionary tendencies of continental margins bordering igneous regions, which form parts of the NAIP, have indicated somewhat diachronous and complex evolution patterns prior to and subsequent to the initiation of the proposed 'main' rifting event at around 55.6 Ma to 56 Ma (Hansen et al., 2009; Brooks, 2011; Larsen et al., 2016; Peace et al., 2017; Franke et al., 2019; Gernigon et al., 2019; Schiffer et al., 2020). When it comes to the driving processes necessary to initiate and maintain tectonic activity associated with momentous events such as the opening of e.g. the N Atlantic and Labrador Sea – Baffin Bay areas in the Early Paleogene Period, some authors have invoked a "bottom-up" mechanism associated with a gigantic ascending mantle plume or a couple of plumes (e.g. Archer et al., 2005; Ganerød et al., 2010; Larsen et al., 2016), while others have argued in favour of a "top-down" mechanism associated with 'continental-drift' and far-field extensional stresses (Peace et al., 2017; Niu, 2020; Niu, 2021). In either case, extension and thinning of the lithosphere must be invoked in order to explain decompression melting and magma transport in sub-vertical dyke systems in the proto Faroe Islands area as well as in other regions of the NAIP prior to, simultaneously and subsequent to the main rifting event at around 55.6 Ma to 56 Ma. Earlier studies on the FIBG have consistently pointed to the formation of the Malinstindur and Enni formations subsequent to a largely quiescent hiatus period with only limited local volcanic activity, which again occurred following deposition of the thick Beinisvørð Formation (e.g. Passey and Jolley et al., 2009 and refs. therein).

### *4.2. Radiometric ages of Faroese sills versus their geochemistry and geography*

When utilising data representing exposed remnants of basaltic sills from the Faroe Islands as indicators on the tectono-magmatic evolution within this region, it is pertinent to bear in mind that the entire Faroese archipelago, currently exposed above sea level, only encompass an area of ~1400 $km_2$ out of the original ~120000 $km_2$ basalt plateau that formed within this region in Paleocene times (e.g. Passey and Jolley, 2009). Hence, hundreds of sills, of which there are no traces left at the present time, could have been emplaced over a geographically wide area at various stages and periods of time during evolution of the original extensive basaltic plateau of the FIBG. Consequently, the remnants of the Faroese sills, as exposed today, may not be entirely indicative of the palaeo igneous activity of the whole region throughout its development, but can act as windows allowing us to examine/interpret the activity of local post-rifting and potential syn-rifting tectono-magmatic events during few and relatively short/restricted periods of time at a few geographic localities.

Altogether, the exposed Faroese sills extend for ~50 km in an ENE-WSW direction and ~20 km in a NNW-SSE direction (Fig. 1). The low-$TiO_2$ and intermediate-$TiO_2$ sills extend to the SSE parts of the area encompassing the actual sills (Hansen, 2011; Hansen et al., 2019), while the bulk of the high-$TiO_2$ sills crop out at a crude ENE-WSW directed trend slightly farther to the NNW in an area that initially was relatively closer to the then neighbouring East Greenland and hence also relatively closer to the axis of initial seafloor-spreading (rifting) between the Faroe Islands and East Greenland in the Early Paleogene Period.

With respect to the Faroese sills, most of these display moderate to noticeable geochemical variations relative to one another, but sill samples within each of two groups, composed of the low-$TiO_2$ Streymoy and Kvívík sills and the high-$TiO_2$ Eysturoy and Sundini sills

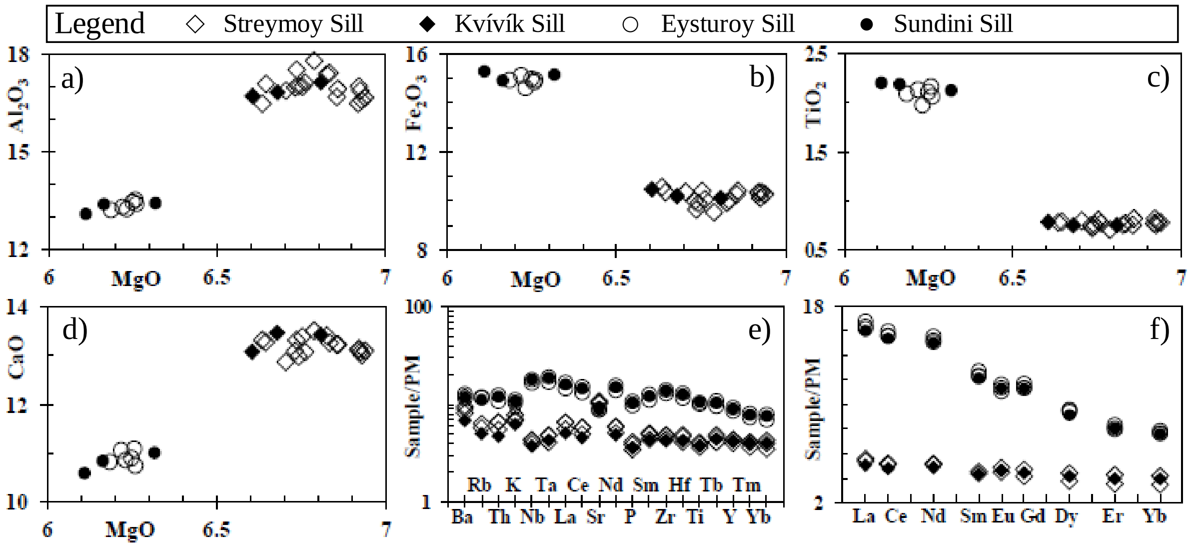


**Figure 3**. The diagrams a) – f) illustrate the close geochemical similarities between the Streymoy and Kvívík sills and between the Eysturoy and Sundini sills respectively (Data from: Hansen, 2011; Hansen et al., 2019). Trace elements and REE are normalised to primitive mantle (PM) values of McDonough and Sun (1995).

respectively, display identical geochemistry/petrography and the two sills within each group also display close spatial relationships (Hansen, 2011; Hansen et al., 2019) (Fig. 1; Fig. 3). Each of the Streymoy Sill and the Eysturoy Sill are by far the most voluminous of the Faroese sills and even more so, when grouped with the Kvívík Sill and the Sundini Sill respectively. Considering the above-mentioned relationships, it is hardly surprising that the Streymoy and Kvívík sills display roughly similar $^{40}Ar/^{39}Ar$ ages with an average of ~55.35 Ma (Table 1; Fig 2). With respect to the high-$TiO_2$ sill group, samples of the Eysturoy Sill display average $^{40}Ar/^{39}Ar$ ages of ~55.35 Ma. It is overwhelmingly likely that the Sundini Sill (dating in progress) formed during that same period of time, considering its intimate geochemical and spatial relationship with the Eysturoy Sill.

It is well established amongst petrologists that high-$TiO_2$ basaltic magmas form at relatively small-degree melting of mantle material, while their low-$TiO_2$ counterparts develop from larger degrees of mantle melting. It is generally acknowledged too that an adiabatic pressure decrease/release in a mantle source above its solidus will lead to increasing degrees of melting, whilst a relative increase in pressure in a mantle source above its solidus at fixed temperatures will result in a relative decrease in the degrees of melting (sub-section 4.6 below). With respect to the large contemporaneous Faroese high-$TiO_2$ Eysturoy and Sundini sills, in addition to the low-$TiO_2$ Streymoy and Kvívík sills (average age ~55.35 Ma), it is worth noting that the average distance between these two contrasting sill groups is only ~13 km and the shortest distance a mere ~6 km (Fig. 1). Another interesting geographical detail on these two sill groups involves the fact that on average the two high-$TiO_2$ sills were emplaced closer to the then active seafloor-spreading axis to the NNW relative to the average distance of their low-$TiO_2$ counterparts.  It is not an uncommon perception within the wider geological society that depths of the lithosphere – asthenosphere boundary and hence mantle depths, where basaltic melts are initiated/formed, in general define depths where high-$TiO_2$ melts and their low-$TiO_2$ counterparts originate, i.e. the former type at relatively great pressures as opposed to lower pressures for the latter (e.g. Niu et al. 2021). It is a general perception too, that depths of lithosphere – asthenosphere boundaries generally increase gradually away from active lithospheric rift axes. If the low-$TiO_2$ and high $TiO_2$ characteristics of the ~55.35 Ma Faroese sills should indeed stem from pressure differences in their mantle sources during formation of their precursor melts, in accordance with gradually decreasing/increasing melting zones, lateral magma transport for considerable distances would have to be invoked for some of these, in addition to the occasional crossing of their respective feeder dykes. A petrogenetic scenario involving melting within a geographically restricted moderately heterogeneous sub-continental lithospheric/asthenospheric mantle, variously affected by previous metasomatic events, has been proposed for these sills earlier (Hansen, 2011; Hansen et al., 2019).

When it comes to the rest of the sills, being dated in this project, it is noticeable that these preserved remnants of the original sills collectively point to a decrease in local melt production during formation of successively younger sills (Svínoy-Fugloy Sill at ~54.45 Ma; Morskranes Sill at ~53.2 Ma; Langaregn and Vestmanna sills at ~50.5 Ma). There are no systematic geochemical trends coupled with variations in radiometric ages of these younger sills. Rather, their precursor magmas were tabbed from moderately heterogeneous mantle sources, where particularly the intermediate-$TiO_2$ Morskranes Sill originated from a noticeably distinct source (e.g. Hansen, 2011; Hansen et al., 2019). Considering the relatively short geographic distances between all exposed Faroese sills, the magmas that gave rise to some of the younger high-$TiO_2$ sills in the actual area could in theory have been tapped from one and the same reservoir, which previously fed the older high-$TiO_2$ Eysturoy and Sundini sills. However, if this was indeed the case, some melt-modifying mechanisms such as replenishing, tapping and/or fractionation (RTF) processes presumably adjusted the geochemical make-up within the actual reservoir(s) in the course of the few myr following the initial tapping of high-$TiO_2$ melts, which gave rise to the Eysturoy and Sundini sills.

*4.3. Geochronology and relationships of Faroese sills and selected host rocks*

In the actual study we utilise a decay constant for $^{40}K$ after Renne et al. (2010) during all geochronology calculations. The age data from this study are compared with relatively recent geochronological data on other samples representing the local lava pile (originally from Storey et al., 2007, which employed $^{40}K$ decay constant of Renne et al., 1998), where we instead make use of recalculated ages by Wilkinson et al. (2016, see caption to Fig.4 for correction details). The recalculated ages in the compilation of Wilkinson et al. (2016), shown to the right of stratigraphic column in Fig. 4, tend to be around 0.6 to 0.65 myr older than those of Storey et al. (2007), hence the extrapolated value shown for the top of the Beinisvørð Formation. The radiometric $^{40}Ar/^{39}Ar$ age of ~56.34 Ma obtained for the lowermost parts of the Malinstindur Formation in this study fits nicely with the recalculated ages for the top of the Beinisvørð Formation at ~57.4 Ma and for the upper parts of the Enni Formation at ~55.8 Ma respectively (Fig. 4). However, if the absolute radiometric ages obtained for both the top of the Beinisvørð Formation and the bottom of the Malinstindur Formation are indeed accurate, it would point to a hiatus period (probably interspersed with

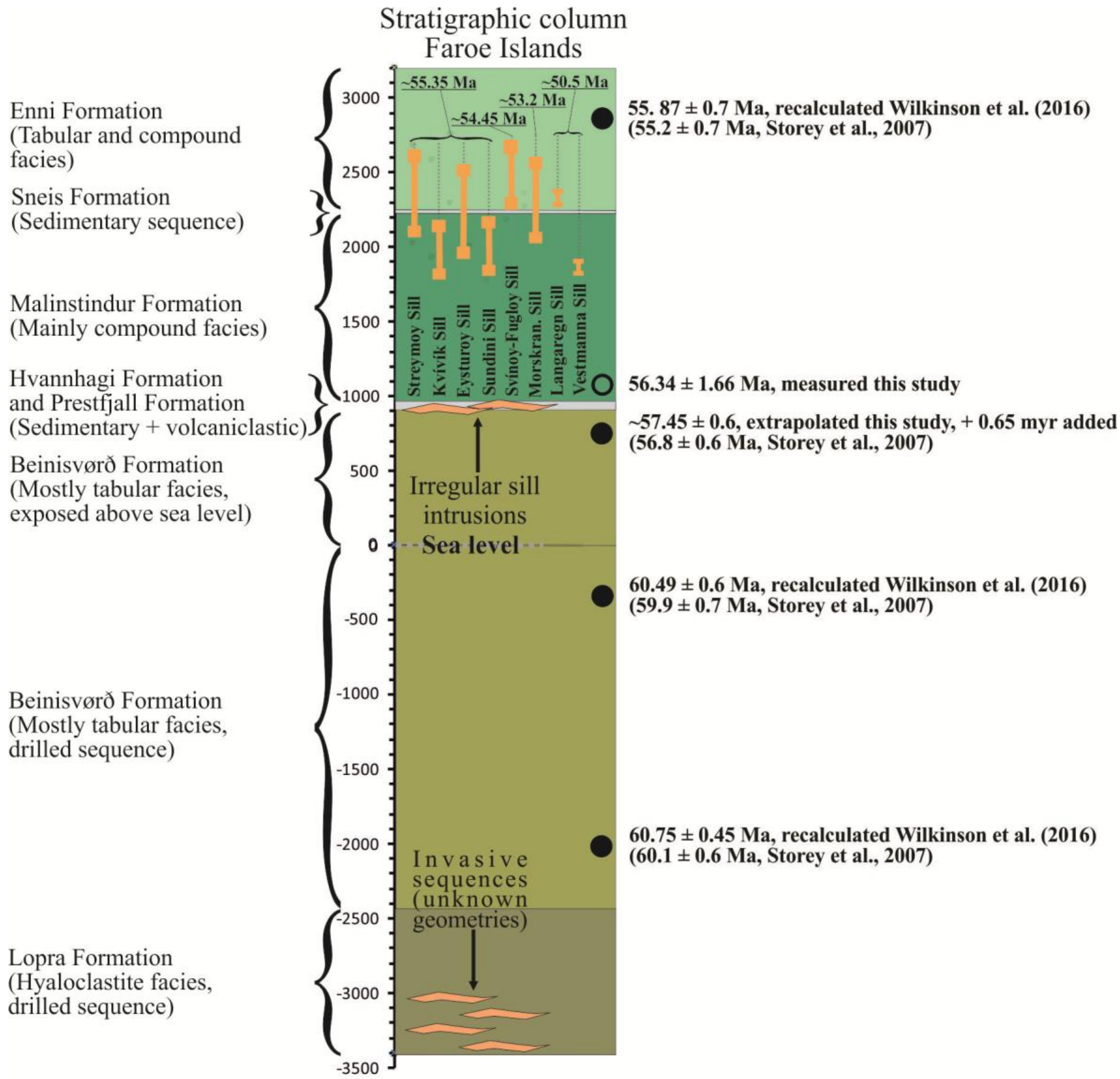


**Figure 4**. $^{40}Ar/^{39}Ar$ radiometric ages of Faroese sills and selected lava formations/sequences are shown in relation to a stratigraphic column representing the basaltic rocks of the Faroe Islands (modified from Fig. 1). Measured sill ages (average values) and age of the local Malinstindur Formation are from this study as presented in Table 1 and Fig. 2. Original ages on Faroese lava formations from Storey et al. (2007) using $^{40}K$ decay constant of Renne et al. (1998) and shown in brackets to the right of the stratigraphic column, have been replaced by recalculated ages in the compilation of Wilkinson et al. (2016) with correction according to Kuiper et al. (2008) and using $^{40}K$ decay constant of Min et al. (2000). Age for top of the Beinisvørð Formation is extrapolated (~0.65 myr added) based on other recalculated data for the actual region by Wilkinson et al. (2016).

shorter periods of limited/sporadic volcanic activity), during which the sedimentary and volcaniclastic Hvannhagi and Prestfjall formations were deposited, which could have lasted for ~1.1 myr.

While the current preserved/exposed rims of Faroese sills are supposed to indicate their original maximum stratigraphic heights fairly accurately (top of orange bars in Fig. 4), the current eroded bottom sections for some of the actual sills could initially have extended to somewhat lower stratigraphic levels than is indicated with the orange bars of the same figure. Apparently, the timing of intrusions did not govern the depths of sill emplacement in the Faroese area to any noticeable degrees, as there are no clear correlation between measured ages for the Faroese sills and their relative positions with respect to geography and stratigraphy, although there exist noticeable degrees of overlap for some sills with respect to their positions/levels in the local stratigraphy (Fig. 1; Fig. 4). In this context it is pertinent to take into account the possibility that the actual area of sill intrusion could have experienced uneven removal of some local strata in the uppermost lava flows in response to erosion during the ~5 million years time-interval between emplacement of the oldest and the youngest sills respectively. In addition, the young Enni Formation could initially have displayed noticeable thickness variations in its top strata that have since been removed by erosion, although the Faroese stratigraphy, as it appears today, is composed of fairly uniform and laterally extensive layers.

Individual intrusions that define three Faroese sill groups of distinct measured ages, were emplaced at different stratigraphic levels initially: 1) The basal and top sections of the two segments of the ~55.35 Ma Streymoy Sill and of the contemporaneous Kvívík Sill display a systematic decrease in stratigraphic elevations from the SE towards the NW (Fig. 5a); 2) The basal and top sections of the two segments of the ~55.35 Ma Eysturoy Sill and of the contemporaneous Sundini Sill display a systematic decrease in stratigraphic elevations from the SE towards the NW (Fig. 5b); 3) The basal and top sections of the ~55.35 Ma Langaregn Sill and of the contemporaneous Vestmanna Sill display a decrease in stratigraphic heights from the SE towards the NW. It is noticeable that volumes for individual sill segments and single sills in the first two of these groups in particular decrease systematically from the SE towards the NW even though no clear differences in their individual geographical/lateral extent is evident, i.e. sill segments and sills generally become successively thinner, more deep-seated stratigraphically and less well developed from the SE towards the NW. Here the SE segment of the Streymoy Sill is 35 – 45 m thick; the NW segment of the same sill is 10 – 30 m thick with the thinnest parts occurring at its preserved basal section towards the WSW while the Kvívík Sill thickens from 0.5 – 1 m at parts of its basal WSW sections to 8 – 10 m at its NE rims. These trends are more or less repeated for the Eysturoy and Sundini sills where the SE segment of the former is 45 – 55 m thick, its NW segment is 10 – 20 m thick and thinning towards its basal WSW sections, while the Sundini Sill is ~0.5 – 1 m thick at its WSW basal sections and reach a maximum thickness of 6 – 8 m at its NE rims.

The characteristics displayed by these two contemporaneous sill groups with increasing

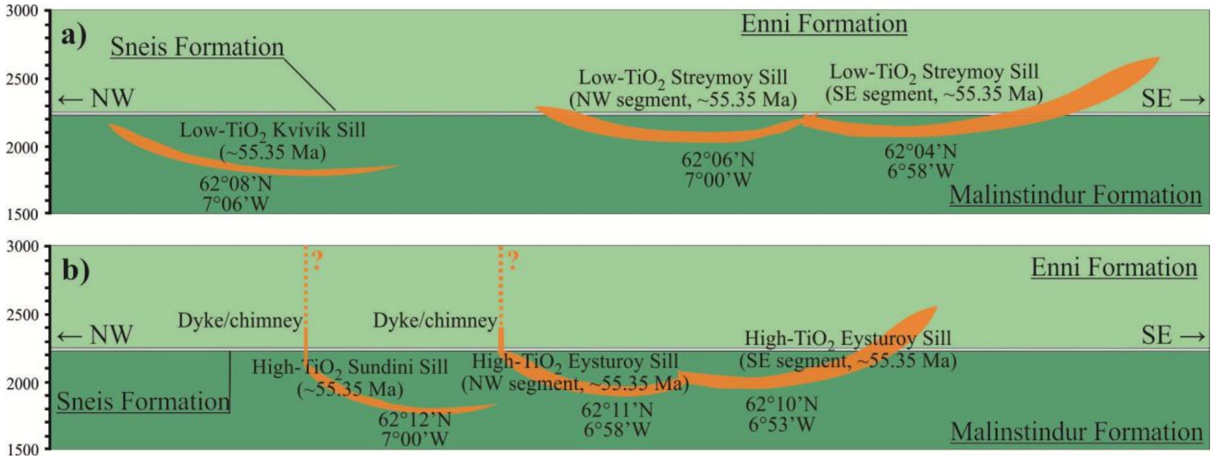


**Figure 5.** The basic drawings illustrate the systematic changes in intrusion depths within two Faroese sill systems (also illustrated in Fig. 1 and Fig. 4), where individual sills and sill segments within each group are of identical ages. Numbers on Y axes refer to the stratigraphic columns shown in Fig. 1 and in Fig. 4. Views are orthogonal to longest sill axes, as these typically appear as elliptical bodies in map view. Average latitudes and longitudes for central sill sections are indicated below each intrusion. a) Longest and shortest axes of these low-$TiO_2$ elliptical sills measure: Streymoy Sill, SE segment, ~5.5 x ~3.5 km; Streymoy Sill, NW segment, ~4.5 x ~2.5 km; Kvívík Sill ~4.5 x ~2.5 km. The sill segments of the Streymoy Sill are connected/welded at their NW and SE extremes respectively, while the shortest (preserved) distance to the Kvívík Sill from the NW segment of the Streymoy Sill is around 2 km in a NW direction. b) Longest and shortest axes of these high-$TiO_2$ elliptical sills measure: Eysturoy Sill, SE segment, ~4 x ~3 km; Eysturoy Sill, NW segment, ~3 x ~3 km; Sundini Sill ~3 x ~3 km. Segments of the Eysturoy Sill are welded at their NW and SE extremes respectively, while the SE parts of the Sundini Sill reaches the NW extreme of the Eysturoy Sill, but occur at a relatively lower altitude. Two sub-vertical dykes/chimneys of limited lateral extent emanate from the highest points of the NW segment of the Eysturoy Sill and the Sundini Sill respectively.

intrusion depths and decreasing sizes/volumes towards the NW could in theory originate from one or more of the following scenarios: i) Their overburdens (i.e. the Enni Formation) systematically decreased in thickness towards the NW at the time of their emplacement, thus resulting in the sills being initiated at successively greater stratigraphic depths towards the NW relative to the Sneis Formation; ii) Intrusion of sills at increasingly deeper crustal levels towards the NW prevented the sills from being fully developed due to impediment from an ever increasing overburden load; iii) Volumes of available magmas, which gave rise to these two sill groups, decreased noticeably from the SE towards the NW thus resulting in intrusions becoming sequentially less well developed; iv) Successive decrease in sill sizes/volumes and their general decrease in developments towards the NW could perhaps result from their initial magmas being channelled right through these still immature intrusions and fed surface magmatism via their uppermost margins for instance. The very restricted lateral extents of preserved dykes/chimneys on top of the Eysturoy and Sundini sills do not indicate transport of large quantities of magmas through these.

*4.4. Pre-rift to syn-rift Faroe Islands versus neighbouring NAIP regions*

As remarked above, the bulk of igneous products associated with the evolution of the NAIP were emplaced during the Early-Middle Paleogene Period. NAIP rocks, emplaced in W Greenland at ~64 Ma to ~28 Ma, were situated ≥1250 km from the then embryonic FIBG in the Early Paleogene Period and had a somewhat complex evolution pattern associated with local extension/rift trajectories (Larsen et al., 2016), while the bulk of the British Tertiary Igneous Province (emplaced at ~64 Ma to ~42 Ma) developed along an extension/rifting trajectory situated well the south and southeast of the FIBG area (e.g. Wilkinson et al., 2016 and refs. therein). Hence, these two NAIP regions are probably not ideally suited when it comes to direct comparison with the contemporaneous FIBG area in general. Other NAIP regions occurring at latitudes roughly matching those hosting the FIBG, like the neighbouring central E Greenland area in particular but perhaps also the N Faroe-Shetland Basin – Møre Marginal High area are supposedly better suited for direct comparisons when it comes to their tectonic and magmatic evolutions in the period of time subsequent to emplacement of lavas forming the uppermost parts of the Beinisvørð Formation. Moreover, coastal areas of central E Greenland, which host the bulk of the NAIP products of this region, display basement thicknesses akin to those determined for the Faroe Islands previously (i.e. Richardson et al., 1998; Darbyshire et al., 2018).

A recent study on offshore basaltic lavas of the N Faroe-Shetland Basin – Møre Marginal High area (including Lagavulin), which were presumably emplaced shortly prior to and perhaps contemporaneously to the inferred main N Atlantic rifting event, tentatively pointed to an origin from multiple local eruption sites and local source areas in response to a main localised rifting event (Walker et al., 2020). These authors argued in favour of initial high-$TiO_2$ magma formation at relatively great mantle depths within the actual area as opposed to generation of their low-$TiO_2$ counterparts in response to melting at shallower mantle levels, which were presumably relatively more affected by regional extension/rifting.

When it comes to FIBG basaltic materials slightly older than those of the Malinstindur and Enni formations (≥55.8 Ma) versus contemporaneous basaltic rocks of the then neighbouring central E Greenland region, it is noticeable that whilst the Faroese area apparently experienced a mostly relatively quiescent/hiatus period with only limited volcanism at ~57.45

Ma to ~56.35 Ma, larger quantities of broadly contemporaneous igneous products were deposited in Blosseville Kyst area, central E Greenland. Examples according to $^{40}Ar/^{39}Ar$ radiometric dating include: Milne Land Fm ~56.8 Ma; Nansen Fjord Fm ~58.4 Ma to ~57.5 Ma (i.e. 58.36 Ma MSWD); Sorgenfri Gletcher diabase/sill ~57.1 Ma; Tobias Dal, Upper Plateau Lava Series ~56.5 Ma (compilation of Wilkinson et al., 2016 and refs. therein). Consequently, it is likely that overall stress regimes (principal stress axes) within these two neighbouring NAIP regions were somewhat dissimilar during that period of time, where 'some' lithospheric extension probably prevailed in parts of the central E Greenland area as opposed to the relatively quiet period without noticeable extensional activity in the contemporaneous FIBG area, i.e. these two regions appear to have been decoupled from one another tectonically during this period of time, or in any case were differently affected by contemporaneous tectonic activity.

Earlier studies have pointed to a probable chemo-stratigraphic association between mostly high-$TiO_2$ basaltic volcanic sequences of central E Greenland (Rømer Fjord Fm and Skrænterne Fm) and the Faroe Islands (Enni Fm), all of which were presumably emplaced shortly prior to the onset of the NE Atlantic rifting (e.g. Søager and Holm, 2009; Millet et al., 2017). Relatively recent high-precision zircon U-Pb geochronological data on the Skaergaard Intrusion of central E Greenland and on the associated Basistoppen Sill point to emplacement ages from ~56 Ma to ~55.85 Ma (Wotzlaw et al., 2012), while gabbros belonging to the oldest part of the neighbouring Kærven Intrusive Complex (gabbro) have yielded $^{40}Ar/^{39}Ar$ ages of around 55.8 Ma (compilation of Wilkinson et al., 2016 and refs. therein). Hence, intrusive activity apparently took place in central E Greenland during the same period of time in which the upper lava sections of the Faroese Enni Formation were emplaced and around 0.3-0.5 myr prior to the onset of intrusive activity in earnest within the Faroese area at ~55.5 Ma (oldest sills emplaced; Fig. 4). Interestingly, $^{40}Ar/^{39}Ar$ radiometric ages on central E Greenland (Blosseville Kyst) lavas of the Rømer Fjord Fm and the Skrænterne Fm, exposed at higher stratigraphic levels when compared to the Skaergaard Intrusion, have yielded ages of ~55.84 Ma (MSWD) and ~55.69 Ma (MSWD) respectively (compilation of Wilkinson et al., 2016 and refs. therein). Accordingly, both surface and intrusive magmatism took place within some parts of central E Greenland (notably the Kangerlussuaq Fjord area) during the same relatively short time span, in which lavas of the relatively young Faroese Enni and Malinstindur formations were emplaced. If younger dykes/chimneys emanating from tops of the NW parts of the Eysturoy Sill and from the Sundini Sill, as shown in Fig. 5, actually fed contemporaneous local surface magmatism, it must have been on a negligible scale due to their restricted lateral extents.

Additional reasons for the recorded mismatch in igneous activity for central E Greenland versus the FIBG respectively at ~56 Ma to ~55.6 Ma could perhaps include: i) The $^{40}Ar/^{39}Ar$ radiometric dating method used in geochronological studies listed above could perhaps be less accurate than the zircon U-Pb dating system in general due to inaccurate $^{40}K$ decay constants (e.g. Naumenko-Dèzes et al. 2018). ii) As the oldest Early Paleogene intrusions of central E Greenland were emplaced partly in top layers of local basement and partly in bottom layers of local lava formations, contemporaneous Faroese intrusive equivalents could in theory reside in none-exposed parts of e.g. the Lopra or Beinisvørð formations. iv) As the current extent of exposed/preserved onshore FIBG lavas represent only minor parts of the initial local lava plateau, intrusions with ages roughly similar to those of the older ones of central E Greenland could in theory have existed within parts of the FIBG, which were later removed by erosion (its NE fringes for instance). However, if the actual recorded/measured data and observations for these two igneous regions do indeed correctly represent igneous events in these two regions at ~56 Ma to ~55.6 Ma, it would appear that the central E Greenland area was affected by short-lived and perhaps repeated fluctuations in sizes and orientations of local principal stress axes shortly prior to the main NE Atlantic rifting event, while more uniform extensional forces prevailed within the FIBG until ~55.6 Ma. Hence, the E Greenland and the Faroese regions or parts of them could in theory have been decoupled tectonically from each other in the time span leading up to the main rifting event in the N Atlantic area too, i.e. sometimes between ~56 Ma to ~55.6 Ma. Causative events that supposedly had the potential to explain the recorded magmatic and hence tectonic mismatches between these two NAIP regions during the actual period of time, could in theory have involved onset of northwards drifting of Greenland relative to the N American and NW European margins, which occurred roughly contemporaneously (e.g. Harrison et al., 1999).

*4.5. Post-rift Faroe Islands versus neighbouring central E Greenland*

It is noticeable that while pre-rift to syn-rift igneous activity within the FIBG occurred exclusively as extrusive magmatism (~61 Ma to ~55.8 Ma), Faroese post-rift igneous activity in turn apparently occurred solely as intrusive magmatism (~55.5 Ma to ~50.5 Ma). Post-rift igneous activity in the then neighbouring central E Greenland region was of a somewhat more diverse nature, comprising both extrusive and intrusive magmatism.

Post-rift volcanic successions emplaced at ~49 Ma to ~44 Ma have been recorded for Kap Dalton, central E Greenland (Blosseville Kyst), along with numerous other lava successions emplaced at ~55.5 Ma to ~53.4 Ma farther to the north along the coast of NE Greenland (compilation of Wilkinson et al., 2016 and refs. therein). Formation of the Kap Dalton lavas in response to a regional rifting event has been envisioned in a previous study (Larsen et al., 2013). Post-rift intrusive activity in central E Greenland include the Kærven Intrusive Complex (alkali granite) emplaced at 53.5 Ma to 53.3 Ma (U-Pb, Thórarinsson et al., 2016); intrusions of the Kialineq District emplaced at 37.9 Ma to 36.9 Ma; intrusions of the Agtertia Fjord lineament and islands intruded at 50.3 Ma to 47.9 Ma; intrusions of the Kangerlussuaq Fjord lineament emplaced at 51.5 Ma to 46.3 Ma and intrusions of the Wiedeman Fjord – Kronborg Gletcher lineament intruded at 52.5 Ma to 37.3 Ma ($^{40}Ar/^{39}Ar$ ages extrapolated from Table 1 of Tegner et al. [2008] by the addition of ~0.7 myr to tabulated values according to recalculations in compilation of Wilkinson et al. [2016], see caption to Fig. 4 above). Hence, the bulk of the post-rift intrusive activity in central E Greenland took place at intervals in the period from ~53.5 Ma to ~37 Ma. Post-breakup intrusive activity in the central E Greenland were previously attributed to re-configuration of NE Atlantic spreading ridges and due to failed continental rift systems in the Kangerlussuaq Fjord region (Tegner et al., 2008).

The actual radiometric age data recorded for Paleocene and Eocene igneous products, being exposed in coastal regions of E Greenland in its entirety, demonstrate that only the extrusive rocks recorded for NE Greenland were emplaced contemporaneous to intrusion of the five oldest and largest basaltic sills of the Faroe Islands. With respect to the contemporaneous central E Greenland region, the lack of recorded radiometric ages for the actual period of time seem to suggest that this particular area could have experienced a relatively quiescent period at ~55.6 Ma to ~53.5 Ma, when it comes to igneous activity. Accordingly, renewed intrusive activity in central E Greenland, which lasted for more than 16 myr altogether, began in earnest broadly contemporaneous to the final stages of intrusive activity in the then neighbouring Faroe Islands. Hence, it appears reasonable to assume that the Faroese and central E Greenland regions were decoupled tectonically/magmatically from one another in the period of time immediately following the onset of the main rifting event in the NE Atlantic and thereafter. While regional rifting events probably governed the subsequent igneous activity in central E Greenland (e.g. Tegner et al., 2008; Larsen et al., 2013), the FIBG area most likely gradually drifted away from areas of active rifting/magmatism to the

WNW in the time span from ~55.5 Ma to ~50.5 Ma and later on as well, as evidenced by the diminishing local igneous activity.

*4.6. Faroese basaltic rocks and seafloor-spreading in the Early Paleogene Period*

The arguments from previous sub-sections seem to suggest that the evolution of the FIBG area during relatively late stages of local Early Paleogene magmatism (i.e. from ~57.4 Ma to ~50.5 Ma), probably occurred in response to regional tectonic events (related to the ultimate rifting of the NE Atlantic), which were not necessary directly associated with those of the then neighbouring regions of the north Faroe-Shetland Basin and the central E Greenland area. On the contrary, events such as: Magmatic activity in central E Greenland while the Faroe Islands experienced a hiatus period (~57.4 Ma - ~56.3 Ma), extrusive and major intrusive activity in central E Greenland while merely extrusive activity took place in the Faroe Islands (~56 Ma - ~55.6 Ma), central E Greenland apparently experienced a hiatus period while noticeable intrusive activity took place in the Faroe Islands (~55.5 Ma - ~53.5 Ma), renewed intrusive activity took place in central E Greenland while intrusive activity rapidly waned in the Faroe Islands (~53.5 Ma - ~37 Ma) all seem to point to two tectonically decoupled regions, which appear to have experienced some kind of alternating magmatism during the time period from ~57.4 Ma to ~50.5 Ma. The notion that the FIBG and central E Greenland igneous regions probably were tectonically decoupled from one another during at least parts of their infancy would be compatible with recent research, suggesting that an ancient microcontinent existed between these two NAIP regions in Early Paleogene times and presumably still exists as a stretched version under the present day Iceland and the Greenland-Iceland-Faroes Ridge (Foulger et al., 2020). The occurrences of a number of Early/Mid Paleogene regional rifting centres, as suggested for central E Greenland (Tegner et al., 2008; Larsen et al 2013) and the northern Faroe-Shetland Basin (Walker et al., 2020), would be in accordance with a recent study on the post-40 Ma NE Greenland region, where several isolated seafloor spreading events/cells presumably triggered local magmatism and the subsequent ultimate main rifting of the NE Atlantic at these latitudes (Franke et al., 2019). In accepting that significant proportions of neighbouring NAIP regions formed in response to regional/local rifting events and that the central E Greenland and Faroese regions probably were tectonically decoupled following emplacement of the Faroese Beinisvørð Formation (at least), it does not appear unrealistic to ascribe the bulk of the magmatic pulses, which built up the Faroe Islands in the Early Paleogene Period (≥ ~57.5 Ma to ≤ ~50.5 Ma), to regional rifting events/pulses, which themselves ultimately developed/coalesced into a common main seafloor-spreading axis in the then embryonic N Atlantic.

General principles on melt production and effusion rates of e.g. basaltic lavas suggest that relatively slow effusion/intrusion rates (compound lava flows, small sills) may be associated with decompression melting at relatively slow extension/spreading rates whilst high(er) effusion/intrusion rates (laterally extensive simple/tabular lava flows, voluminous sills) are indicative of fast(er) extension/spreading rates (Walker, 1971; Harris and Rowland, 2009). Accordingly, the mostly compound lavas of the Malinstindur Formation (Passey and Jolley, 2009 and refs. therein) point to relatively sluggish extension/spreading rates during its formation (from ~56.34 Ma). In addition to compound flows, the common occurrences of thick simple/tabular lavas in the Enni Formation (+ Sneis Fm.), suggest increased rates of melting and extension/spreading towards the end of surface magmatism period/event within the Faroe Islands at around ~55.8 Ma (Table 1 and Fig. 4). Hence, provided that the radiometric ages determined for the Malinstindur and Enni formations are indeed accurate/reliable, these two formations, in addition to the Sneis Formation, probably came into being during a total time span of only ~0.5 myr in total. Rather than sharing common mantle sources, geochemical similarities between the Skrænterne and Rømer Fjord formations of central E Greenland with those of e.g. the contemporaneous Faroese Enni Formation could in theory well reflect similarities in extension rates within their respective mantle sources during melting, thus resulting in broadly similar igneous products.

Obviously, the entire nature of magmatism in the FIBG region changed radically from the cessation of surface magmaticm at ~55.8 Ma and to the onset of sill emplacement at ~55.5 Ma, presumably triggered by reorientations of regional principal stress axes or changes of their magnitudes (i.e. previous sections). Apparently, the Faroese region experienced a relatively short hiatus period of ~0.3 myr lasting from cessation of local extrusive activity until the onset of local intrusive activity.

Recent research on the north Faroe-Shetland Basin region pointed to an initial regional line of breakup located ~50 km to the NNW off the Faroe Islands in the Early Paleogene Period (Walker et al., 2020). Accordingly, the oldest Faroese sills (The low-$TiO_2$ Streymoy and Kvívík sills; the high-$TiO_2$ Eysturoy and Sundini sills) were emplaced ~75 km from the incipient seafloor spreading axis on average. If an average spreading rate of ~0.013 m per year for the last ~56 myr is accepted for the eastern fringes of the evolving N Atlantic rift system, the distances to the active rift system of the younger Faroese sills during their emplacement were: For the Svínoy-Fugloy Sill (average age ~54.4 Ma) the distance was around 89.3 km; for the Morskranes Sill (age ~53.2 Ma) the distance was approximately 104.9 km and the Vestmanna and Langaregn sills (average age ~50.5 Ma) were on average emplaced 140 km from the active rifting axis. Consequently, the observed decrease in sill sizes/volumes with decreasing ages reflect a decrease in local igneous activity with increasing distances to the active N Atlantic rift system, i.e. lithospheric extension rates within the actual region apparently abated gradually and finally came to a more or less standstill in the matter of ~5 to 5.3 myr following initial breakup. In this context it is worth noticing, that an absence of mutual alignments between recorded dykes that initially fed the Faroese sills or between dykes/chimneys emanating from a few of these point to very modest or perhaps a near-absence of extension-related stress fields in the uppermost crust during their intrusions. The sills themselves however, did of course generate compression-related stresses in the host basalts upon their vigorous intrusions and subsequent evolvements (Hansen in prep.).

*4.7. Early Paleogene Faroese mafic melts and potential mantle depths of origin*

When it comes to basaltic lavas and intrusive rocks of various ages building up the various regions of the NAIP, these are customarily grouped into high-$TiO_2$ versus low-$TiO_2$ basaltic compositions. The former are commonly interpreted to have formed by low-degree melting of suitable mantle material at noticeable depths (i.e. at relatively high pressure), while the latter are often interpreted to have formed by larger degrees of mantle melting at shallower mantle depths (i.e. at relatively low pressure). A few recent studies, dealing with the petrogenetic evolutions of basaltic rock suites of the Faroe Islands and those of another neighbouring NAIP region at the NW European margin, utilised these $TiO_2$ criteria to distinguish between genesis of basaltic magmas at deep versus more shallow mantle levels respectively (Millet et al., 2017; Millet et al., 2020; Walker et al., 2020). Such interpretations/models generally rely on the assumption that the base of the actual lithosphere was more or less smooth with continuous and gradual transitions between thick and thinner lithosphere, following its extension and stretching. In reality however, the lithosphere – asthenosphere boundary (LAB), the depth of which is generally thought to be important for the extent of mantle melting to produce basaltic magmas (Niu, 2021), may in reality vary noticeably over relatively short geographical distances in some igneous regions, depending on their previous tectonic histories (Peace et al., 2017; Darbyshire et al., 2018; Rychert et al., 2020). In the context of high-$TiO_2$ versus low-$TiO_2$ compositions in basaltic magmas, it is pertinent to note that $TiO_2$ contents in such magmas are not particularly sensitive to pressure during melting, but rely chiefly on the degrees of melting of suitable sources, where $TiO_2$

contents decrease with increasing degrees of melting irrespective of ambient pressure conditions (Kinzler, 2017; Collinet et al., 2015). An example of the formation of high-$TiO_2$ (incompatible element enriched) basaltic magmas at shallow crustal levels, includes incompatible element enriched horizons within the Skaergaard Intrusion, central E Greenland, which reportedly formed in response to low-percentage remelting of hydrothermally altered older basaltic rocks of this renowned intrusion (Wotzlaw et al., 2012). Also, $TiO_2$ contents in basaltic magmas remain relatively stable during moderate percentages of fractional crystallisation from these of e.g. plagioclase and pyroxenes (e.g. Hansen et al., 2019). Source fertility and content of fluids in the actual sources, in addition to ready supply of heat so as to increase local temperatures govern overall melting percentages (Table 2). In turn, temperatures required to reach some local solidus ($T_S$) or temperatures in excess of the local solidus ($T_E$) can be gained by either heat supply from lower local stratigraphic levels at fixed pressures within the melting area or by local adiabatic upwelling so as to initiate or maintain local decompression melting (e.g. Niu, 2021).

With respect to the degrees of melting necessary, in order to produce basaltic magmas of variable $TiO_2$ compositions, a relatively wide span in melting percentages of slightly heterogeneous mantle sources (5% to 7.5% and 16% to 21% respectively) were required in order to explain the relatively wide compositional ranges recorded for both high-$TiO_2$ and low-$TiO_2$ samples representing basaltic sills of the Faroe Islands (Hansen et al., 2019). A

**Table 2.** Changes in solidus temperatures, melt percentages and major element compositions as functions of changes in physical conditions during formation of basaltic magmas by mantle melting.

| | [a, b]Increasing fertility (basaltic material added?) | [c; d; e; f]Increasing temperature (fixed pressure) | [a; e; f, g]Increasing pressure (fixed temperature) | [b; f; g, h]Increasing % melting (fixed temp. and press.) | [h; i]Increasing fluid/$H_2O$ content (Metasomatism?) |
|---|---|---|---|---|---|
| Solidus | Decreasing $P_O$ | ------------ | Increasing $P_O$ | ------------ | Decreasing $P_O$ |
| Melt % | Increasing | Increasing | Decreasing | ------------ | Increasing |
| $SiO_2$ | ------------ | [j]Decreasing - [k]Increasing | Decreasing | [l]Decreasing - [m]Increasing | ------------ |
| $Al_2O_3$ | ------------ | decreasing | ------------ | Decreasing | decreasing |
| $FeO_{tot}$ | Increasing | Increasing | Increasing | Increasing | Increasing |
| MgO | ------------ | Increasing | ------------ | Increasing | Increasing |
| CaO | ------------ | [j]Increasing - [k]Decreasing | ------------ | [l]Increasing - [m]Decreasing | ------------ |
| $Na_2O$ | ------------ | Decreasing | ------------ | Decreasing | ------------ |
| $TiO_2$ | ------------ | Decreasing | Slight increase | Decreasing | ------------ |

Superscript letters from a to i point to studies of: [a]Yaxley (2000); [b]Kogiso et al. (1998); [c]Baker and Stolper (1994); [d]Ulmer (2001); [e]Falloon et al. (2008); [f]Kinzler, 1997; [f]Collinet et al. (2015); [g]Hirose and Kushiro (1993); [h]Hirose and Kawamoto (1995); [i]Green and Falloon (2005). [j]Valid at temperatures below ~1350° C; [k]Valid at temperatures above ~1350° C; [l]Valid at melting percentages lower than ~15%; [m]Valid at melting percentages larger than ~15%. $P_O$ refer to pressure (GPa) at solidus.

significantly greater/wider span in melting percentages of slightly heterogeneous mantle sources would be required in order to explain $TiO_2$ ranges, recorded for samples of the Faroese Beinisvørð Formation in a recent study (Millet et al., 2020). Melting percentages in the range of ~5 ± 1% of suitable mantle sources are commonly invoked for the production of high-$TiO_2$ basaltic melts (e.g. Hansen et al., 2019 and refs. therein). Accordingly, a vertical mantle column of around 50 kilometres covering a considerable geographical extent would be required so as to produce the ~2.5 km high-$TiO_2$ main/middle section of the Beinisvørð Formation in response to ~5% mantle melting of asthenospheric peridotite. Substantial additional melting would be required in order to produce the remaining high-$TiO_2$ basaltic rocks of the Faroe Islands similar melting percentages. When it comes to geochemical "evidences" on presumed formation of basaltic melts within the garnet-lherzolite stability field at relatively "deep" mantle levels, recent research has suggested that spinel- and plagioclase-lherzolite pooled and near-fractionated melts of compositionally and thermally variable peridotites best produce the highly variable trace element and isotope garnet signatures commonly encountered in such melts (Krein et al., 2020). Compositionally variable xenoliths representing the SCLM from a number of central European localities, which experienced extension earlier in their geological history, are commonly intensely metasomatised by alkali basaltic melts or silica-saturated to oversaturated basaltic melts, formed by low-percentage melting within the underlying asthenospheric mantle (Patkó et al., 2020; Puziewicz et al., 2020). Consequently, upper parts of the asthenosphere and lower parts of the SCLM in areas, which were exposed to e.g. extension/rifting during previous geological events, are frequently laced with metasomatic agents such as low-percentage asthenosphere-derived alkali or silica saturated basaltic melts, which commonly solidified prior to reaching equilibrium with their host rocks, thus contributing substances to surrounding mantle materials that possessed solidus temperatures lower than those typical of surrounding mantle levels. Extension across ancient suture zones that are related to previous tectonic events, which was commonplace during formation of the NAIP, is thought to have the potential of redistributing lithospheric material to the asthenosphere by eroding it from lower levels of the local SCLM and ultimately redistributing it in the underlying regional asthenosphere (Foulger et al., 2020). To sum up, the abovementioned compositional variations in certain zones of the asthenospheric mantle, which may be affected by incorporated metasomatic agents such as alkali and/or silica saturated/oversaturated basaltic materials, in addition to potential inclusion of metasomatised slices of SCLM materials, could in theory have served as seeds/nucleus possessing solidus temperatures lower than those of

the average uncontaminated asthenosphere, thus triggering initial mantle melting and subsequent rifting in response to lithospheric extension within regions the NAIP.
All things considered the question arise, would it be a realistic scenario to invoke only 'deep' mantle asthenospheric sources/levels for all high-$TiO_2$ basaltic rocks of the Faroe Islands (i.e. a black and white scenario) or, should low-percentage melting at shallower mantle levels to produce high-$TiO_2$ magmas be considered a viable alternative too? Implicit in this topic is the additional question: did regional-scale fluctuations in mantle temperatures, which originated from deeper mantle levels, account for variations in effusion rates being recorded for extensional-related igneous regions like those of the NAIP or, did these result from repeated extension-related adiabatic ascents of mantle materials that shifted relative temperatures locally so as to cause them to cross local solidus temperatures?

*4.8. Lithosphere configuration and potential origin of Early Paleogene Faroese magmas*

With respect to basaltic rocks of the Faroe Islands, high-$TiO_2$ and low-$TiO_2$ lavas occur as intimately associated and alternating layers in numerous localities (Passey and Jolley, 2009; Søager and Holm, 2011; Millet et al., 2017; Millet et al., 2020), thus indicating a direct spatial and temporal relationship, i.e. in broad concurrence with the characteristics displayed by the four oldest Faroese sills (Hansen, 2011; Hansen et al., 2019), as pointed out in previous sub-sections. In order to properly constrain the general petrogenetic history of basaltic rocks like those of the Faroe Islands by means of their $TiO_2$ contents for instance, it would be advantageous to address mantle architectures as related to geography, which have the potential to noticeably influence geochemical compositions of basaltic magmas in general.
When it comes to lithosphere thicknesses and general LAB geometries in the North Atlantic area during the Early Paleogene Period, previous studies have pointed to the probable existence of ancient suture zones from previous tectonic events in literally all of the igneous regions of the NAIP, including the FIBG area (Hansen et al., 2009; Hansen, 2011; Peace et al., 2017; Foulger et al., 2020; Gernigon et al., 2020; Schiffer et al., 2020).
Consequently, it doesn't appear unreasonable to infer irregular LAB geometries, comparable to those presented by Rychert et al. (2020) for instance, for some of the igneous regions, which formed part of the NAIP in the Early Paleogene Period (Fig. 6a and Fig. 6b). Scenarios like those displayed in Fig. 6 suggest that mantle environments with uneven LAB geometries have the potential to generate melts of various geochemical compositions, during periods with lithospheric extension/thinning and associated adiabatic mantle upwelling and

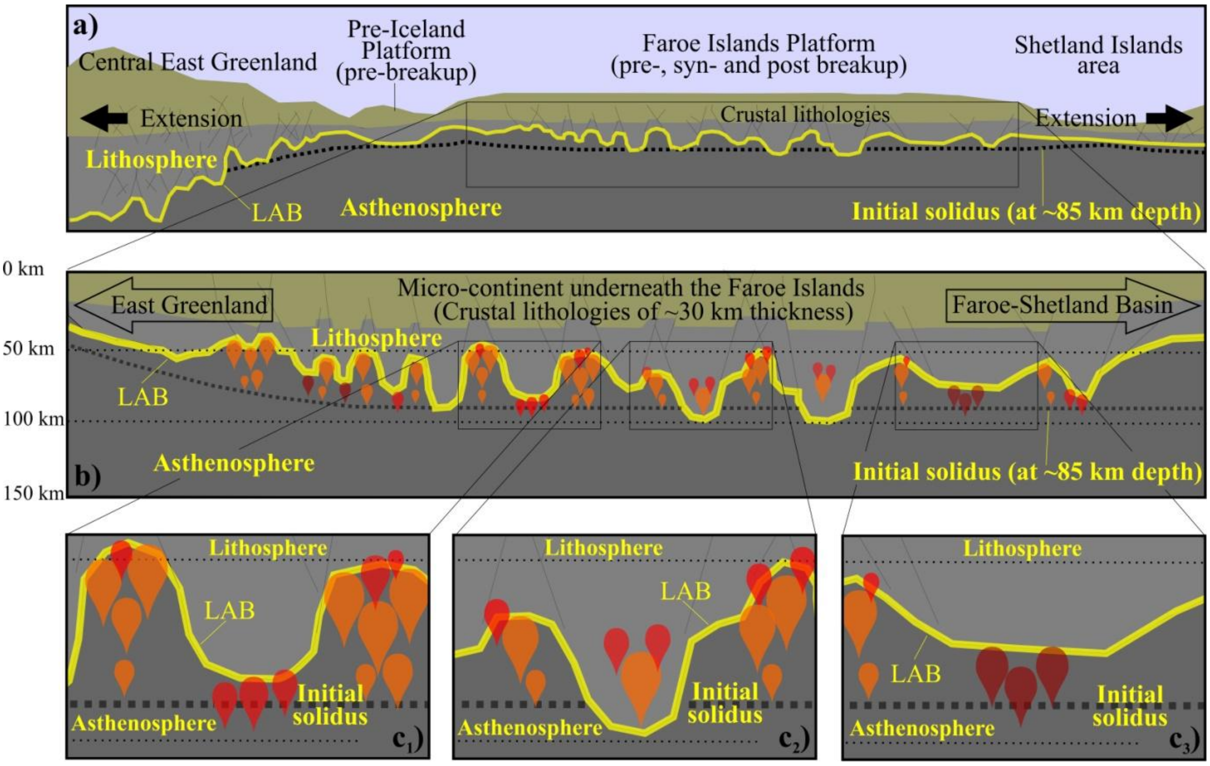


**Figure 6.** Profiles indicating idealised lithosphere-asthenosphere boundaries (LAB) in the E. Greenland, Iceland, Faroe Islands and Shetland Islands regions in the Early Paleogene Period (modified general LAB geometries from Rychert et al., 2020). Inverted reddish droplets indicate low-percentage high-$TiO_2$ melts, vine-red droplets indicate moderate-percentage intermediate-$TiO_2$ melts, while inverted orange droplets point to relatively large-percentage low-$TiO_2$ melts. a) The entire proto Faroe Islands area was affected by the extension between E Greenland and the NW European margin in the Early Paleogene Period. b) Extension/stretching across the Faroe Islands Platform in the Early Paleogene Period triggered widespread decompression melting at mantle levels between solidus and the LAB, thus leading to the formation of high-$TiO_2$ and low-$TiO_2$ magmas. $c_1$) The lid effect could have resulted in the formation of low-percentage high-$TiO_2$ melts at relatively deep mantle levels and higher-percentage low-$TiO_2$ melts at shallower mantle levels. Adiabatic ascent of noticeable quantities of low-$TiO_2$ magmas could have triggered low-percentage melting of particularly fertile surrounding mantle materials to produce additional low-percentage high-$TiO_2$ melts at relatively shallow mantle lewels. In addition, one would expect a noticeable spread in $TiO_2$ compositions in large individual batches of magmas. $c_2$) Partly as in $c_1$, but with additional inferred melting in the sub-continental lithospheric mantle. $c_3$) Partly as in $c_1$, but also with the production of intermediate-$TiO_2$ melts from moderate-percentage melting at moderately deep mantle levels.

decompression melting. In the tentative model(s) presented in Fig. 6b and Fig. 6c, high-$TiO_2$ basaltic melts are ideally formed by low-percentage melting at relatively great mantle depths within relatively restricted vertical melting intervals, whilst their low-$TiO_2$ counterparts ideally formed by relatively high-percentage melting at relatively shallow mantle depths within a relatively wide vertical melting interval. We further envisage (tentatively) that high-

$TiO_2$ basaltic magmas from low-percentage melting of mantle materials and/or unterplated basaltic materials, originating from earlier local igneous episodes, occasionally formed at the peripheries of (and in response to) large volumes of hot low-$TiO_2$ basaltic magmas, pooling in the neighbourhood of local LAB beneath the Faroese area in the Early Paleogene Period (Fig. 6b and Fig. 6c). In point of fact, a suitable analogue here would be the incompatible element-enriched basaltic rocks recorded for parts of the Skaergaard Intrusion, E Greenland, which formed by remelting of some of its older parts in the presence of trace amounts of fluids, in response to intrusive activity associated with the emplacement of the adjacent basaltic Basistoppen Sill (Wotzlaw et al., 2012). Formation of basaltic magmas from melting of fertile mantle sources and/or mantle sources variously affected by previous melting and/or metasomatising events in e.g. deep keels of the sub-continental lithospheric mantle (SCLM) beneath the Faroese area in the Early Paleogene Period, as visualised in Fig. 6b and Fig. $6c_2$, remain potential options when it comes to production of high-$TiO_2$ and low-$TiO_2$ melts at mantle depths, which did not necessarily differ noticeably between sources to these two categories, (i.e. discussion above and e.g. Hansen, 2011; Hansen et al., 2019).

Altogether, the tentative inferences presented above for Early Paleogene production of basaltic magmas with various $TiO_2$ compositions in the mantle underneath the developing FIBG offer a few alternative explanations in addition to already existing petrogenetic theories. Moreover, alternative petrogenetic processes/mechanisms like these within the actual area in the Early Paleogene Period would negate the requirements for huge quantities of lateral magma transport, through the upper mantle or lower/middle crust for tens (or hundreds?) of kilometres prior to their eruptions/intrusions at broadly similar localities. When it comes to magma transport in the upper mantle, it is worth bearing in mind that: i) Well established physical facts state that silicate melts are less dense and more voluminous than the melted proportions of their source rocks in e.g. the Earth's upper mantle; ii) The mantle itself is expected to become less strong with decreasing depths/pressures (i.e. at ≤ 48 km, e.g. Katayama, 2021); iii) Both the relative decrease in gravity of melts versus their melted source-rocks and the ambient pressure gradient will act to effectively drain newly formed melts upwards from their mantle sources; iv) unless ascending mafic magmas encounter substantial obstructions such as thick impregnable and laterally extensive rock layers, which effectively cap an area of magma ascent, these should be expected to preferably drain upwards rather than venture for long lateral distances prior to reaching the upper crust. Consequently, under normal circumstances the sub-vertical components of magma transport in the upper mantle and lower crust should expectedly be larger than any associated lateral components.

With respect to the oldest of the contemporaneous high-$TiO_2$ and low-$TiO_2$ sill groups of the FIBG, their close spatial relationships in addition to their geochemical compositions, led Hansen et al. (2019) to suggest that their origins were not necessarily linked to the lid effect, but that they rather developed by melting of neighbouring mantle sources variously affected by metasomatism, i.e. in accordance with Fig. $6c_2$. Of the younger sills, only the Morskranes Sill is an intermediate-$TiO_2$ type, while the rest are of the high-$TiO_2$ category. All of these younger sills could have formed directly underneath the young Faroese lava plateau, with the Morskranes Sill forming at moderately deep mantle levels in response to moderate-percentage mantle melting, while the younger high-$TiO_2$ sills could have formed by low-percentage mantle melting in accordance with one of the options shown in Fig. 6. It is clear from geochemical compositions however, that the Langaregn Sill (~50.5 Ma) could have formed at deeper mantle levels when compared to the rest of the Faroese sills, perhaps at the spinel lherzolite - garnet lherzolite boundary (Hansen et al., 2019).

The tentative hypotheses presented here regarding the bulk of Faroese igneous products initially developing from local magma sources rather than from more distant ones, suggest that chemostratigraphically similar basaltic sequences of the FIBG and East Greenland do not necessarily originate from common mantle sources, as has been tentatively suggested earlier (e.g. Søager and Holm, 2009; Millet et al., 2017 and refs, therein). Indeed, age comparisons between these two igneous regions (presented in sub-section 4.6 above) suggest noticeable contemporary differences with respect to their regional stress regimes and magmatic emplacement styles subsequent to ~57.5 Ma at any rate. Hence, a contemporary Iceland microcontinent, as suggested by Foulger et al. (2020), could readily have been accommodated between the Faroe Islands and central E Greenland according to our hypothesis. An alternative mechanism, which has the potential to explain observed chemostratigraphical similarities between a few contemporaneous basaltic sequences within these two NAIP regions (i.e. Enni formation, FIBG, versus Skrænterne and Rømer Fjord formations central E Greenland), would be identical extension rates that resulted in identical effusion rates from melting of broadly similar mantle sources.

## 5. Summary and concluding remarks

In this contribution we present new $^{40}Ar/^{39}Ar$ ages for most of the sills exposed on the Faroe Islands, in addition to new and recalculated $^{40}Ar/^{39}Ar$ ages for some of the Faroese basaltic lava formations. Altogether, novel measured radiometric ages and compiled recalculated radiometric ages suggest that the basaltic rocks of the Faroe Islands formed in a time interval from ~61 Ma to ~50.5 Ma, i.e. it took at least ~10.5 myr for the initial Faroese basaltic plateau and its intrusive systems to develop. As no reliable measured ages are available for the Faroese Lopra Formation yet, the Faroe Islands could potentially be a few hundred thousand years older than the currently recorded maximum ages. Based on the geochronological results obtained in this study, a few inferences regarding timing and sequences of events within the FIBG and in the then neighbouring central E Greenland region during the Early Paleogene Period, can be presented:

1. Following outpourings of basaltic hyaloclastic material in a shallow-marine and/or in a marshy sub-aerial environment to build up the lowermost Lopra Formation of the Faroe Islands at ≥ ~61 Ma the overlying Beinisvørð Formation came into being between ~61 Ma and ~57.45 Ma (~3.55 myr in total) in response to emplacement of significant quantities of magmas hosted mostly in tabular lava flows, i.e. quite likely during a time span with noticeable rates of extension/effusion.
2. The Presthagi and Hvannhagi formations, which reside on top of the Beinisvørð Formation and are composed of sedimentary and pyroclastic sequences, were deposited during a prolonged hiatus period lasting from ~57.4 to ~56.2 Ma (~1.2 myr in total), according to geochronological of this contribution.
3. From the bottom up the Malinstindur, the Sneis and the Enni formations, which rest atop Presthagi and Hvannhagi formations, formed from ~56.35 Ma to ~55.85 Ma, i.e. within the relatively narrow time interval of ~0.5 myr, where local extension/effusion rates presumably increased during formation/deposition of the latter two formations.
4. Subsequent to the deposition of the presumed top layers of the Enni Formation at ~55.85 Ma, changes in the regional stress fields triggered the formation of relatively voluminous basaltic intrusives in the form of the Streymoy, Kvívík, Eysturoy and Sundini sills at ~55.5 Ma to ~55.2 Ma (average ~55.35 Ma). Successively less voluminous saucer-shaped basaltic sills were intruded into the Faroese lava pile at ~54.75 Ma to ~54.05 Ma (Svínoy-Fugloy Sill, average ~54.4 Ma); at ~53.15 Ma (Morskranes Sill) and at ~50.7 Ma to ~50.3 Ma (Langaregn and Sundini sills, average ~50.5 Ma).

With respect to mantle sources, the melting of which gave rise to the igneous products of the Early Paleogene Period that built up the Faroese region, a few petrogenetic models have been presented in earlier contributions, all of which have the potential to explain a great deal of the observed and measured characteristics of the FIBG. However, in this contribution we point to the additional possibility of basaltic melt formation in a mantle environment with an irregular lithosphere-asthenosphere boundary (LAB) configuration, where melt generation at various mantle depths adjacent to the LAB provide the low-$TiO_2$, intermediate-$TiO_2$ and the high-$TiO_2$ basaltic rock types encountered in the archipelago of the Faroe Islands. We envisage general transport of molten rocks, which initially built up Faroese lavas and sills, via multiple feeder systems, which in turn were supplied from multiple magma sources generated over relatively wide geographic areas within the FIBG region.

*Future works*: It would be desirable to acquire some additional $^{40}Ar/^{39}Ar$ radiometric ages representing of a few Faroese lava horizons, notably from the Beinisvørð, Malinstindur, Sneis and Enni formations within the foreseeable future, in addition to supplementary radiometric ages on a few local sills.

*Disclaimer*: The authors declare that they have no conflict of interest and nothing to disclaim.

**Acknowledgements**

Assistance from a few relatives and local residents of the village of Miðvágur, Faroe Islands, with respect to the financing of costs associated with laboratory and other expenses are much appreciated. An earlier version of the manuscript benefitted from constructive critique by an anonymous senior geologist. Reviews by two anonymous reviewers are appreciated.

**References**

Abrahamsen, N. (2006). Palaeomagnetic results from the Lopra-1/1A re-entry well, Faroe Islands. *Geological Survey of Denmark and Greenland Bulletin*, **9**, 51-65.

Á Horni, J. A., Hopper, J. R., Blischke, A., Geisler, W. H., Stewart, M., McDermott, K. H., Judge, M., Erlendsson, Ö. and Árting, U. E. (2017). Regional distribution of volcanism within the North Atlantic Igneous Province. *Geological Society, London, Special Publications*, **447**, 105-125. http://doi.org/10.1144/SP447.18

Archer, S. G., Bergman, S. C., Iliffe, J., Murphy, C. M. and Thornton, M. (2005). Palaeogene igneous rocks reveal new insights into the geodynamic evolution and petroleum potential of the Rockall Trough, NE Atlantic Margin. *Basin Research*, **17**, 171-201. doi:10.1111/j.1365-2117.2005.00260.x

Baker, M. B. and Stolper, E. M. (1994). determining the composition of high-pressure mantle melts using diamond aggregates. *Geochimica et Cocmochimicia Acta*, **58**(13), 2811-2827.

Brooks, C. K. (2011). The East Greenland rifted volcanic margin. *Geological Survey of Greenland and Denmark Bulletin*, **24**, pp. 97.

Collinet, M., Medard, E., Charlier, B., Auwera, J. V. And Grove, T. L. (2015). Melting of the primitive martian mantle at 0.5–2.2 GPa and the origin of basalts and alkaline rocks on Mars. *Earth and Science Planetary Letter*, **427**, 83-94. https://doi.org/10.1016/j.epsl.2015.06.056

Darbyshire, F. A., Dahl-Jensen, T., Larsen, T. B., Voss, P. H. and Joyal, G. (2018) Crust and uppermost-mantle structure of Greenland and the Northwest Atlantic from Rayleigh wave group velocity tomography. *Geophysical Journal International*, **212**, 1546–1569. doi: 10.1093/gji/ggx479

Falloon, T. J., Green, D. H., Danyushevsky, L. V. and McNeill, A. W. (2008). The composition of near-solidus partial melts of fertile peridotite at 1 and 1.5 GPa: implications for the petrogenesis of MORB. *Journal of Petrology*, **49**(4), 591-613.

Foulger, G. R., Doré, T., Emeleus, C. H., Franke, D., Geoffroy, L., Gernigon, L., Hey, R., Holdsworth, R. E., Hole, M., Höskuldsson, Á., Julian, B., Kusznir, N., Martinez, F., McCaffrey, K. J. W., Natland, J. H., Peace, A. L., Petersen, K,. Stephenson, R. and Stoker, M. (2020). The Iceland Microcontinent and a continental Greenland-Iceland-Faroe Ridge. *Earth-Science Reviews*, **206**, 102926. https://doi.org/10.1016/j.earscirev.2019.102926

Franke, D., Klitzke, P., Barckhausen, U., Berglar, K., Berndt, C., Damm, V., Dannowski, A., Ehrhart, A., Engels, M., Funck, T., Geissler, W., Schnabel, M., Thorwart, M. and Trinhammer. P. (2019). Polyphase magmatism during the formation of the northern East Greenland continental margin. *Tectonics*, **38**(4), 2961-3982. doi.10.1029/2019TC005552

Ganerød, M., Smethurst, M. A., Torsvik, T. H., Prestvik, T., Rousse, S., McKenna, C., Van Hinsbergen, D. J. J. and Hendriks, B. W. H. (2010). The North Atlantic Igneous Province reconstructed and its relation to the Plume Generation Zone: the Antrim Lava Group revisited. *Geophysical Journal International*, **182**(1), 183-202. http://doi.org/10.1111/j.1365-246X.2010.04620.x

Gernigon, L., Franke, D., Geoffroy, L., Schiffer, C., Foulger, G. R. and Stoker, M. (2020). Crustal fragmentation, magmatism, and the diachronous opening of the Norwegian-Greenland Sea. *Earth-Sciences Reviews*, **206**(102839), 1-37. https://doi.org/10.1016/j.earscirev.2019.04.011

Green, D. H. and Falloon, T. J. (2005). Primary magmas at mid-ocean ridges, ”hotspots,” and other intraplate settings: Constraints on mantle potential temperature. in Foulger GR, Natland JH, Presnall DC, Anderson DL, eds., Plates, plumes, and paradigms: *Geological Society of America Special Paper*, **388**, 217-247.

Hansen J. (2011). Petrogenetic Evolution, Geometries and Intrusive Styles of the Early Cenozoic Saucer-Shaped Sills of the Faroe Islands. *Doctoral thesis, Durham University*. http://etheses.dur.ac.uk/3631/

Hansen J. (2015). A numerical approach to sill emplacement in isotropic media: Do saucer-shaped sills represent ‘natural’ intrusive tendencies in the shallow crust? *Tectonophysics*, **664**, 125–138. http://dx.doi.org/10.1016/j.tecto.2015.09.006

Hansen, J. (2020). Transgressive sills and lateral lava flows: on the visual observation of igneous sheets in rugged mountainous terrains and the optical illusion factor. *Earth Sciences*, **9**(5), 164-177. doi :10.11648/j.earth.20200905.13

Hansen, J., Davidson, J. P., Jerram, D. A., Ottley, C. J. and Widdowson, M. (2019). Contrasting $TiO_2$ compositions in Early Cenozoic mafic sills of the Faroe Islands: an example of basalt formation from distinct melting regimes. *Earth Sciences*, **8**(5), 235-267. http://www.sciencepublishinggroup.com/j/earth doi: 10.11648/j.earth.20190805.11

Hansen, J. and Ganerød, M. (2022). Geochronology of the Faroe Islands: A case study on $^{40}Ar/^{39}Ar$ dating of local basaltic sills and selected lavas. *Mendeley Data*, **V2**, doi: 10.17632/87gtjjh5gb.2

Hansen, J., Jerram, D. A., McCaffrey, K. J. W. and Passey, S. R. (2009). The onset of the North Atlantic Igneous Province in a rifting perspective, *Geological Magasine*, **146**(3), 309-325. https://doi.org/10.1017/S0016756809006347

Harris, A. J. L. and Rowland, S. K. (2009). Effusion rate controls on lava flow length and the role of heat loss: A review. From: THORDARSON, T., SELF, S., LARSEN, G., ROWLAND, S. K. & HOSKULDSSON, A. (eds) Studies in Volcanology: The Legacy of George Walker. Special Publications of IAVCEI, 2, 33– 51. Geological Society, London. 1750-8207/09/$15.00 # IAVCEI 2009. https://doi.org/10.1144/IAVCEl002.3

Harrison, J. C., Mayr, U., McNeil, D. H., Sweet, A. R., McIntyre, D. J., Eberle, J. J., Harington, C. R., Chalmers, J. A., Dam, G. and Nøhr-Hansen, H. (1999). Correlation of Cenozoic sequences of the Canadian Arctic region and Greenland; implications for the tectonic history of northern North America. *Bulletin, Canadian Petroleum Geology*, **47**(3), 223-254.

Hirose, K. and Kushiro, I. (1993). Partial melting of dry peridotites at high pressures: Determination of compositions of melts segregated from peridotite using aggregates of diamond. *Earth and Planetary Science Letters*, **114**, 477-489.

Hirose, K. and Kawamoto, T. (1995). hydrous partial melting of lherzolite at 1 GPa: The effect of $H_2O$ on the genesis of basaltic magmas. *Earth and Planetary Science Letters*, **133**, 463-473.

Holm, P. M., Hald, N. and Waagstein, R. (2001). Geochemical and Pb-Sr-Nd isotopic evidence for separate hot depleted and Iceland plume mantle sources for the Paleogene basalts of the Faroe Islands, *Chemical Geology*, **178**, 95-125. https://doi.org/10.1016/S0009-2541(01)00260-1

Jolley, D. W. and Bell, B. R. (2002). The evolution of the North Atlantic Igneous Province and the opening of the NE Atlantic Rift. *Geological Society, London, Special Publications*, **197**, 1-13.

Katayama, I. (2021). Strength models of the terrestrial planets and implications for their lithospheric structure and evolution. *Progress in Earth and Planetary Science*, **8**(1), pp. 17, https://doi.org/10.1186/s40645-020-00388-2

Kinzler, R. J. (1997). Melting of mantle peridotite at pressures approaching the spinel to garnet transition: Application to mid-ocean ridge basalt petrogenesis. *Journal of Geophysical Research*, **102**(B1), 853-874. https://doi.org/10.1029/96JB00988

Kuiper, K. F., Deino, A., Hilgen, F. J., Krijgsman, W., Renne, P. R. and Wijbrans, J. R. (2008). Synchronizing rock clocks of Earth history.Science, **320**(5875), 500-504. https://doi.org/10.1126/science.1154339

Kogiso, T., Hirose, K. and Takahashi, E. (1998). Melting experiments on homogeneous mixtures of peridotite and basalt: application to the genesis of ocean island basalts. *Earth and Planetary Science Letters*, **162**, 45-61.

Krein, S. B., Behn, M. D. and Grove, T. L. (2020). Origins of major element, trace element and isotope garnet signatures in mid-ocean ridge basalts. *Journal of Geophysical Research: Solid Earth*, **125**(12), https://doi.org/10.1029/2020JB019612

Larsen, L. M., Pedersen, A. K., Sørensen, E. V., Watt, W. S. and Duncan, R. A. (2013). Stratigraphy and age of the Eocene Igtertivâ Formation basalts, alkaline pebbles and sediments of the Kap Dalton Group in the graben at Kap Dalton, East Greenland. ©2013 by Bulletin of the Geological Society of Denmark, Vol. 61, pp. 1–18. ISSN 2245-7070. (www.2dgf.dk/publikationer/bulletin). https://doi.org/10.37570/bgsd-2013-61-01

Larsen, L. M., Pedersen, A. K., Tegner, C., Duncan, R. A., Hald, N. and Larsen, J. G. (2016) Age of Tertiary volcanic rocks On the West Greenland Continental Margin: volcanic evolution and event correlation to other parts of the North Atlantic Igneous Province. *Geological Magazine*, **153**, 487-511. doi.10.1017/S0016756815000515

Lee, J-Y,. Marti, K., Severinghaus, J. P, Kawamura, K., Yoo, H-S., Lee, J. B. and Kim, J. S. (2006). A redetermination of the isotopic abundances of atmospheric Ar. *Geochimica et Cosmochimica Acta*, **70**, 4507-4512. doi:10.1016/j.gca.2006.06.1563

McDonough, W. F. and Sun, S.-s. (1995). The composition of the Earth. *Chemical Geology*, **120**, 223-253.

McDougall, I. and Harrison, T. M. (1999). Geochronology and Thermochronology by the $^{40}$Ar/$^{39}$Ar Method. *Oxford University Press*, pp. 269.

Millett, J. M., Hole, M. J., Jolley, D. W. and Passey, S. R. (2017). Geochemical stratigraphy and correlation within Large Igneous Provinces: The final preserved stages of the Faroe Islands Basalt Group, *Lithos*, **286–287**, 1-15. https://doi.org/10.1016/j.lithos.2017.05.011

Millet, J. M., Hole, M. J., Jolley, D. W., Passey, S. R. and Rosetti, L. (2020). Transient mantle cooling linked to regional volcanic shut-down and early rifting in the North Atlantic Igneous Province. *Bulletin of Volcanology*, **82:61**, pp. 27. https://doi.org/10.1007/s00445-020-01401-8

Min, K., Mundil, R., Renne, P. R., and Ludwig, K. R. (2000). A test for systematic errors in $^{40}$Ar/$^{39}$Ar geochronology through comparison with U/Pb analysis of a 1.1-Ga rhyolite. Geochimica et Cosmochimica Acta, 64(1), 73-98. https://doi.org/10.1016/S0016-7037(99)00204-5

Meyer, R., Van Wijk, J. and Gernigon, L. 2007. The North Atlantic Igneous Province: A review of models for its formation. *Geological Society of America*, *Special Paper* **430**, 525-52.

Naumenko-Dèzes, M. O., Nägler, T. F., Mezger, K. and Villa, M. (2018). Constraining the 40K decay constant with $^{87}$Rb-$^{87}$Sr – $^{40}$K-$^{40}$Ca chronometer intercomparison. *Geochimica et Cosmochimica Acta*, 220, 235-247. https://doi.org/10.1016/j.gca.2017.09.041

Niu, Y. (2020). On the cause of continental breakup: A simple analysis on driving mechanisms of plate tectonics and mantle plumes. *Journal of Asian Earth Sciences*, **194**, 104367. http://doi.org/10.1016/j.jseaes.2020.104367

Niu, Y. (2021). Lithosphere thickness controls the extent of mantle melting, depth of melt extraction and basalt compositions in all tectonic settings on Earth – A review and new perspectives. *Earth-Science Reviews*, **217**(103614), pp. 25. https://doi.org/10.1016/j.earscirev.2021.103614

Passey, S. R. and Jolley, D. W. (2009). A revised lithostratigraphic nomenclature for the Palaeogene Faroe Islands Basalt group, NE Atlantic Ocean. *Earth and Environmental Science Transactions of the Royal Society of Edinburg*, **99**, 127-158.

Patkó, L., Liptai, N., Aradi, L. E., Klébesz, R., Sendula, E., Bodnar, R. J., Kovács, I. J., Hidas, K., Cesare, B., Novák, A., Trásy, B. and Szabó. (2020). Metasomatism-induced wehrlite formation in the upper mantlebeneath the Nógrád-Gömör Volcanic Field (Northern Pannonian Basin): Evidence from xenoliths. *Geoscience Frontiers*, **11**(3), 943-964. https://doi.org/10.1016/j.gsf.2019.09.012

Puziewicz, J., Matusiak-Malek, M., Ntaflos, T., Grégoire, M., Kaszmarek, M-A., Aulbach, S., Ziobro, M. and Kukula, A. (2020). Three major types of subcontinental lithospheric mantle beneath the Variscan Orogen in Europe. *Lithos*, **362-363**, 105467. https://doi.org/10.1016/j.lithos.2020.105467

Peace, A. L., Foulger, G. R., Schiffer, C. and McCaffrey, K. J. W. (2017). Evolution of Labrador Sea–Baffin Bay: Plate or Plume Processes? *Geoscience Canada*, **44**, 91-102. https://doi.org/10.12789/geocanj.2017.44.120

Renne, P. R., Mundil, R., Balco, G., Min, K. and Ludwig, K. R. (2010). Joint determination of $^{40}K$ decay constants and $^{40}Ar*/^{40}K$ for the Fish Canyon sanidine standard, and improved accuracy for $^{40}Ar/^{39}Ar$ geochronology. *Geochimica et Cosmochimica Acta*, **74**(18), 5349-5367. https://doi.org/10.1016/j.gca.2010.06.017

Renne, P. R., Swisher, C. C., Deino, A. L., Karner, D. B., Owens, T. L. and DePaolo, D. J. (1998). Intercalibration of standards, absolute ages and uncertainties in 40Ar/39Ar dating. *Chemical Geology*, **145**, 117-152.

Richardson, K. R., Smallwood, J. R., White, R. S., Snyder, D. B. and Maguire, P. K. H. (1998). Crustal structure beneath the Faroe Islands and the Faroe-Iceland Ridge, *Tectonophys*, **300**, 159-180. https://doi.org/10.1016/S0040-1951(98)00239-X

Rychert, C. A., Harmon, N., Constable, S. and Wang, S. (2020). The Nature of the Lithosphere-Asthenosphere Boundary. *Journal of Geophysical Research: Solid Earth*, **125**, e2018JB016462, pp. 39, DOI: 10.1029/2018jb016463

Saunders, A. D. (2016). Two LIPs and two Earth-system crises: the impact of the North Atlantic Igneous Province and the Siberian Traps on the Earth-surface carbon cycle. *Geological Magazine*, **153**(2), 201–222. doi:10.1017/S0016756815000175

Saunders, A. D., Fitton, J. G., Kerr, A. C., Norry, M. J. and Kent, R. W. (1997). The North Atlantic Igneous Province. *Geophysical Monograph* **100**, 45–93.

Schiffer, C., Doré, A. G., Foulger, G. R., Franke, D., Geoffroy, L., Gernigon, L., Holdsworth, B., Kuznir, N., Lundin, E., McCaffrey, K., Peace, A. L., Petersen, D., Phillips, T. B., Dtephenson, R., Stoker, M. and Welford, J. K. (2020). Structural inheritance in the North Atlantic. *Earth-Science Reviews*, **206**(102975). https://doi.org/10.1016/j.earscirev.2019.102975

Storey, M., Duncan, R. A. and Tegner, C. (2007). Timing and duration of volcanism in the North Atlantic Igneous Province: implications for geodynamics and links to the Iceland hotspot. *Chemical Geology*, **241**, 264-281. doi:10.1016/j.chemgeo.2007.01.016

Svensen, H., Planke, S. And Corfu, F. (2010) Zircon dating ties the NE Atlantic sill emplacement to initial Eocene global warming. *Journal of the Geological Society, London*, **167**, 433-436. doi.1144/0016-76492009-125

Søager, N. and Holm, P. M. (2009). Extended correlation of the Paleogene Faroe Islands and East Greenland plateau basalts. *Lithos*, **107**, 205-215. https://doi.org/10.1016/j.lithos.2008.10.002

Søager, N. and Holm, P. M. (2011). Changing compositions of the Iceland plume; Isotopic and elemental constraints from the Paleogene Faroe flood basalts, *Chemical Geology*, **280**, 297-313. https://doi.org/10.1016/j.chemgeo.2010.11.017

Thórarinsson, S. B., Holm, P. M., Tappe, S., Heaman, L. M. and Prægel, N-O. (2016) U–Pb geochronology of the Eocene Kærven intrusive complex, East Greenland: constraints on the Iceland hotspot track during the rift-to-drift transition. *Geological Magazine*, **153**(1), 128-142. DOI: https://doi.org/10.1017/S0016756815000448

Tarling, D. H. and Gale, N. H. (1968). Isotopic dating and palaeomagnetic polarity in the Faeroe Islands. *Nature*, **218**, 1043-1044.

Tegner, C., Brooks, C. K., Duncan, R. A., Heister, L. E. and Bernstein, S. (2008). $^{40}Ar/^{39}Ar$ ages of intrusions in East Greenland: Rift-to-drift transition over the Iceland hotspot. *Lithos*, **101**, 480-500. https://doi.org/10.1016/j.lithos.2007.09.001

Tegner, C., Duncan, R. A., Bernstein, S., Brooks, C. K., Bird, D. K. and Storey, M. (1998). $^{40}Ar/^{39}Ar$ geochronology of Tertiary mafic intrusions along the East Greenland rifted margin: relation to flood basalts and the Iceland hotspot track. *Earth and Planetary Science Letters*, **156**, 75-88. https://doi.org/10.1016/S0012-821X(97)00206-9

Ulmer, P. (2001). Partial melting inj the mantle wedge – the role of $H_2O$ in the genesis of mantle-derived ’arc-related’ magmas. *Physics of the Earth and Planetary Interiors*, **127**, 215-232. https://doi.org/10.1016/S0031-9201(01)00229-1

Waagstein, R. (1988). Structure, composition and age of the Faeroe basalt plateau. *Geological Society, London ,Special Publications*, **39**, 225-238. https://doi.org/10.1144/GSL.SP.1988.039.01.21

Waagstein, R., Guise, P. and Rex, D. (2002). K/Ar and $^{40}Ar/^{39}Ar$ whole-rock dating of zeolite facies metamorphosed flood basalts: the upper Paleocene basalts of the Faroe Islands, NE Atlantic. *Geological Society, London, Special Publications*, **197**, 219-252.

Walker, G.P.L. (1971). Compound and simple lava flows and flood basalts. *Bulletin Volcanologique*, **35**, 579-590. https://doi.org/10.1007/BF02596829

Walker, F., Schofield, N., Millet, J., Jolley, D., Hole, M. and Stewart, M. (2020). Paleogene volcanic rocks in the northern Faroe–Shetland Basin and Møre Marginal High: understanding lava field stratigraphy. *Geological Society, London, Special Publications*, **495**, https://doi.org/10.1144/SP495-2019-13

Wilkinson, C. M., Ganerød, M., Hendriks, B. W. H. and Eide, E. A. (2016). Compilation and appraisal of geochronological data from the North Atlantic Igneous Province (NAIP). *Geological Society, London, Special Publications*, **447**, http://doi.org/10.1144/SP447.10

Wotzlaw, J-F., Bindeman, I. N., Schaltegger, U., Brooks, C. K. and Naslund, H. R. (2012). High-resolution insights into episodes of crystallization,hydrothermal alteration and remelting in the Skaergaard intrusive complex. *Earth and Planetary Science Letters*, **255-256**, 199-212. DOI: 10.1016/J.EPSL.2012.08.043

Yaxley, G. M. (2000). Experimental study of the phase and melting relations of homogeneous basalt + peridotite mixtures and implications for the petrogenesis of flood basalts. *Contributions to Mineralogy and Petrology*, **139**, 326-338.